the plant journal SEB

*The Plant Journal* (2020) doi: 10.1111/tpj.14751

# Light regulation of light-harvesting antenna size substantially enhances photosynthetic efficiency and biomass yield in green algae†

**Sangeeta Negi[1], Zoee Perrine[2], Natalia Friedland[3], Anil Kumar[2], Ryutaro Tokutsu[4,5,6], Jun Minagawa[4,5,6], Howard Berg[2], Amanda N. Barry[7], Govindjee Govindjee[8] and Richard Sayre[9,*]**

[1]*New Mexico Consortium and Los Alamos National Laboratory, Los Alamos, NM 87544, USA,*
[2]*Donald Danforth Plant Science Center, St. Louis, MO 63132, USA,*
[3]*Stanford University, Palo Alto, CA, USA,*
[4]*Division of Environmental Photobiology, National Institute for Basic Biology, 38 Nishigonaka, Myodaiji, Okazaki 444-8585, Japan,*
[5]*Department of Basic Biology, School of Life Science, The Graduate University for Advanced Studies (SOKENDAI), 38 Nishigonaka, Myodaiji, Okazaki 444-8585, Japan,*
[6]*CREST (Core Research for Evolutional Science and Technology), Japan Science and Technology Agency (JST), 38 Nishigonaka, Myodaiji, Okazaki 444-8585, Japan,*
[7]*Los Alamos National Laboratory, Los Alamos, NM 87544, USA,*
[8]*Department of Biochemistry, Department of Plant Biology, Center of Biophysics and Quantitative Biology, University of Illinois at Urbana-Champaign, Urbana, IL 61801, USA, and*
[9]*New Mexico Consortium, Los Alamos, NM 87544, USA*

Received 5 September 2019; revised 6 February 2020; accepted 9 March 2020.
*For correspondence (e-mail richardtsayre@gmail.com).
†This paper is dedicated to the memory of Mark Hildebrand, a pioneer in diatom molecular biology and photosynthesis.

## SUMMARY

**One of the major factors limiting biomass productivity in algae is the low thermodynamic efficiency of photosynthesis. The greatest thermodynamic inefficiencies in photosynthesis occur during the conversion of light into chemical energy. At full sunlight the light-harvesting antenna captures photons at a rate nearly 10 times faster than the rate-limiting step in photosynthetic electron transport. Excess captured energy is dissipated by non-productive pathways including the production of reactive oxygen species. Substantial improvements in photosynthetic efficiency have been achieved by reducing the optical cross-section of the light-harvesting antenna by selectively reducing chlorophyll *b* levels and peripheral light-harvesting complex subunits. Smaller light-harvesting antenna, however, may not exhibit optimal photosynthetic performance in low or fluctuating light environments. We describe a translational control system to dynamically adjust light-harvesting antenna sizes for enhanced photosynthetic performance. By expressing a chlorophyllide *a* oxygenase (*CAO*) gene having a 5′ mRNA extension encoding a Nab1 translational repressor binding site in a CAO knockout line it was possible to continuously alter chlorophyll *b* levels and correspondingly light-harvesting antenna sizes by light-activated Nab1 repression of CAO expression as a function of growth light intensity. Significantly, algae having light-regulated antenna sizes had substantially higher photosynthetic rates and two-fold greater biomass productivity than the parental wild-type strains as well as near wild-type ability to carry out state transitions and non-photochemical quenching. These results have broad implications for enhanced algae and plant biomass productivity.**

**Keywords: *Chlamydomonas*, algae, photosynthesis, light-harvesting antenna, chlorophyll, thylakoid, non-photochemical quenching, biofuels.**

## INTRODUCTION

One of the major challenges facing future generations is the sustainable production of food, fiber, and fuels on increasingly limited and degrading arable lands (Lauk and Lutz, 2016). By the end of this century, the human global population is estimated to increase from 7.4 to 11 billion. By 2050, virtually all non-protected arable land (20% of total land mass) is expected to be under cultivation. Meeting the challenge of increasing demand for food, fuel, and fiber to sustain the growing population requires substantial increases in agricultural productivity. One potential approach to address this challenge is to increase the photosynthetic efficiency and biomass productivity of primary biomass producers including microalgae and terrestrial plants (Subramanian *et al.*, 2013; Ort *et al.*, 2015).

Photosynthetic efficiencies in plants and algae range from 1 to 5% of available solar energy (Long *et al.*, 2006; Ducat and Silver, 2012; Subramanian *et al.*, 2013; Ort *et al.*, 2015). Theoretically, however, photosynthetic efficiencies as high as 11% are feasible using solar energy (Long *et al.*, 2006). There are several metabolic targets that can be modified to improve this efficiency. These targets can be broadly be categorized into those associated with inefficiencies in light capture and energy conversion processes, the biochemistry of $CO_2$ fixation and associated carbon metabolism, and metabolic feedback inhibition associated with end-product accumulation and ultimately crop yield sink strength (Subramanian *et al.*, 2013; Ort *et al.*, 2015). Although the maximum efficiency for the conversion of chlorophyll (Chl) excited states into charge-separated states by the photosynthetic reaction center complexes and their associated electron-transport processes has been reported to be 83.2% (Bjorkman and Demmig, 1987), almost 80% of the energy captured by Chl and associated pigments is lost as heat or fluorescence at maximum solar light (Ort *et al.*, 2011; Perrine *et al.*, 2012). At full sunlight intensities, Chls of the light-harvesting antenna complexes (LHC) of plants and green algae capture photons at a rate that is approximately 10 times faster (0.1 msec) than the rate-limiting step (*c.* 1 msec) in photosynthetic electron transport, that is the oxidation of plastoquinol ($PQH_2$) by the cytochrome $b_6f$ complex (Witt, 1971; Whitmarsh and Govindjee, 1995). These rate limitations coupled with the lack of sufficient electron buffering capacity in the electron-transport system (PQ and cytochrome $b_6f$ complex pool sizes) necessary to accommodate $PQH_2$ oxidation kinetics leads to the saturation of photosystem II (PSII) electron transport at high solar light intensities. Over-reduction of the PSII electron acceptors in turn leads dissipation of excess energy captured by LHC as heat, Chl fluorescence, and through the production of potentially damaging singlet oxygen species (Ohad *et al.*, 1992; Niyogi, 1999; Ruffle *et al.*, 2001; Subramanian *et al.*, 2013; Berman *et al.*, 2015; Demmig-Adams *et al.*, 2016). During 80% of the day the photosynthetic electron-transport system of plants and green algae is light saturated leading to the non-productive dissipation of excess captured energy and reducing the collective photosynthesis of the system (e.g. in a plant canopies or in algae ponds) (Niyogi, 1999; Müller *et al.*, 2001; Niinemets, 2016; Friedland *et al.*, 2019).

One strategy to increase light use efficiency is to reduce the loss of Chl excited states through non-productive energy dissipation pathways. Reduction in non-productive energy dissipation pathways can be achieved by reducing the optical cross-section of the LHC so that the rate of photon capture is more closely coupled to downstream rate limitations in electron transfer (Ort *et al.*, 2011; Perrine *et al.*, 2012; Blankenship and Chen, 2013; Cazzaniga *et al.*, 2014). A variety of strategies have been developed to optimize light-harvesting antenna sizes for more efficient light utilization. These include reduction in total Chl (*a* and *b*) and carotenoid content per chloroplast or cell, targeted reduction in the abundance of specific light-harvesting antenna subunits, and selective reduction in Chl *b* levels leading to a reduction in the peripheral light-harvesting antenna optical cross-section (Polle *et al.*, 2003; Kirst *et al.*, 2012; Mitra *et al.*, 2012; Perrine *et al.*, 2012; Mussgnug *et al.*, 2007; Beckman *et al.*, 2009; Cazznigga *et al.*, 2014; Friedland *et al.*, 2019). For example, algae having reductions in multiple LHC pigment-protein subunits have been shown to have higher photosynthetic quantum efficiencies than wild-type algae (Mussgnug *et al.*, 2007). However, these strains had no apparent advantage in growth or biomass yield relative to their wild-type parental lines. These results indicate that simultaneous and large reductions in multiple peripheral antenna complex subunits did not enhance biomass yields (Mussgnug *et al.*, 2007; de Mooij *et al.*, 2015). Similar results have been observed for algae in which only the peripheral LHC proteins were reduced in abundance. Strains with reduced LHC levels had both increased sensitivity to high light intensities as well as reduced photosynthetic rates under subsaturating light intensities (Beckmann *et al.*, 2009; Oey *et al.*, 2013; Wobbe and Remacle, 2015; Kromdijk *et al.*, 2016).

Other strategies to manipulate light-harvesting antenna sizes have been less targeted. For example, inactivation of the *tla1* gene (Polle *et al.*, 2003) resulted in a 70% reduction in total Chl/ cell (Mitra *et al.*, 2012). Similarly, the TAM (truncated antenna mutant) mutants in *Chlorella sorokiniana* were shown to have reduced Chl content per cell. Interestingly, one of the TAM mutants (TAM-2) showed higher light use efficiency at saturating irradiance resulting in a 30% increase in biomass when grown in outdoor photobioreactors (Cazzaniga *et al.*, 2014). Overall, it has been observed that mutants having truncated light-harvesting antenna sizes require higher light intensities than wild-type


*The Plant Journal*, (2020), doi: 10.1111/tpj.14751

algae to achieve similar photosynthetic rates. In addition, these mutants generally produced less biomass than their wild-type parental strains when grown in dense cultures where light is limiting (Formighieri *et al.*, 2012; de Mooij *et al.*, 2015).

Another strategy used to manipulate light-harvesting antenna size is to alter the accumulation of Chl *b* (Polle *et al.*, 2000; Perrine *et al.*, 2012). Reductions in Chl *b* accumulation impacts light-harvesting antenna size by selectively reducing the abundance of the peripheral LHC subunits that bind *c.* 75% of the total Chl and 100% of the Chl *b*. This selective reduction in LHC abundance is because in plants and green algae, only the LHC family members bind Chl *b*, while the reaction centers and associated inner antenna subunits (e.g. CP43 and CP49 for PSII) bind only Chl *a* (Hoober *et al.*, 2007). During the assembly of the peripheral LHC complexes, individual LHC subunits are imported into the chloroplast and folded in the presence of pigments. LHC proteins lacking sufficient Chl *b* are structurally destabilized and degraded (Hoober *et al.*, 2007). Thus, reduction in Chl *b* levels leads to selective reduction of peripheral LHC complex members and not to reduction in the Chl *a* containing, proximal antenna proteins (e.g. CP43 and CP47 of PSII) most closely coupled to the photosystems.

In addition to harvesting light, the peripheral light-harvesting antenna plays an important role in mediating and balancing energy distribution between the two photosystems (state transitions) and in dissipating excess captured energy through non-photochemical quenching (NPQ) processes (Müller *et al.*, 2001; Minagawa, 2011; Ruban, 2015). Thus, while the elimination of the peripheral LHC complexes would substantially reduce the kinetic constraints between rates of light capture and energy conversion, the complete elimination of peripheral LHC complexes would be expected to reduce efficiencies in whole chain electron transport due to impairment in the ability to carry out state transitions, increases in susceptibility to photodamage associated with impaired NPQ processes, and reduced photosynthetic rates at subsaturating light intensities. Consistent with this hypothesis, the complete elimination of the Chl *b* and peripheral LHCs has been shown to substantially reduce growth rates in algae and plants (Blankenship *et al.*, 2011; Perrine *et al.*, 2012; de Mooij *et al.*, 2015).

Taking these observations into consideration potential strategies to maximize photosynthetic efficiency should: (1) maximize the conversion of photons into photochemically charge-separated states, (2) optimize energy redistribution and balance between the two photosystems (state transitions) under high light intensities, (3) support NPQ activity at saturating light intensities to reduce photodamage, and (4) respond to changing light conditions to maximize the efficiency of light capture and energy conversion throughout the day (Mircovic *et al.*, 2016).

Previously, we have demonstrated that *Chlamydomonas reinhardtii* cells, having intermediate light-harvesting antenna sizes, meet many of these criteria (Perrine *et al.*, 2012). Cells with intermediate antenna sizes (Chl *a*/*b* ratio *c.* 5) had photosynthetic rates at saturating light intensities that were 40% greater than wild-type parental strains and had little reduction in the capacity to carry out state transitions and NPQ (Perrine *et al.*, 2012). By partially suppressing chlorophyllide *a* oxygenase (CAO) activity, the chloroplastic enzyme that catalyzes the two-step oxygenation reaction of chlorophyllide *a* into chlorophyllide *b,* a 30% reduction in LHCII trimer complexes was observed (Tanaka *et al.*, 1998; Eggink *et al.*, 2004; Perrine *et al.*, 2012). Similar enhanced photosynthetic phenotypes were observed in *Camellia* plants with altered Chl *b* levels. Similar to algae, the optimal photosynthetic performance and biomass yield in engineered *Camelina* was observed at a Chl *a*/*b* ratio of 5 (Friedland *et al.*, 2019). However, these *CAO* RNAi engineered organisms (algae and plants) had a range of fixed-size LHCs and thus were limited in their ability to optimize light utilization in changing light environments and stratified light gradients. Similar to the light-intensity gradients observed from the top to the bottom of plant canopies, light intensities in algal ponds fluctuate constantly during the day associated with alterations in solar intensity as well as changes in algal culture density and mixing. Perrine *et al.* (2012) suggested that by dynamically regulating light-harvesting antenna size to maximize the efficiency of light utilization it would be possible to reduce non-productive energy dissipation and maximize biomass productivity. Here we demonstrate that algae capable of dynamically adjusting their peripheral light-harvesting antenna size in response to changing light intensities have substantial improvements in photosynthetic efficiency and effective light stress responses leading to substantially enhanced biomass accumulation relative to wild-type algae in fluctuating light environments. The increases in biomass production observed by modulating the size of the light-harvesting antenna size are among the largest improvements observed to date.

## RESULTS

### Engineering an adjustable light-harvesting antenna system

To achieve dynamic control of light-harvesting antenna size, we took advantage of a well known light-regulated translational repressor of gene expression, the NAB1 protein. NAB1 protein abundance and activity in *Chlamydomonas* is light regulated transcriptionally and post-translationally by the redox state of the cells and increases in activity with increasing light intensity (Wobbe *et al.*, 2009). Our target for modulating the physical size of the


*The Plant Journal*, (2020), doi: 10.1111/tpj.14751

light-harvesting antenna was the manipulation of Chl *b* synthesis. To modulate Chl *b* levels, we designed a modified *CAO* gene that included 13 bases of the NAB1-binding, light responsive motif (LRE) of the *LHCMB6* gene fused to the 5′ end of the *CAO* gene (Figure 1) (Mussgnug *et al.*, 2007; Wobbe *et al.*, 2009). The expression of the *LRE–CAO* construct was driven by the strong light-regulated *PSAD* promoter and terminator to achieve the greatest possible dynamic range of CAO expression (Kumar *et al.*, 2013). To avoid background *CAO* expression and Chl *b* synthesis, the LRE–*CAO* expression cassette was introduced into a *CAO* knockout mutant (*cbs3*) of *Chlamydomonas reinhardtii* (Figure 2a,b) (Tanaka *et al.*, 1998). Transgenic algae (designated by NC) expressing the LRE–*CAO* construct are expected to have high NAB1 translational repressor activity when grown at high light intensities; this then leads to reduced translation of LRE–*CAO* mRNA resulting in lower Chl *b* levels and reduced peripheral light-harvesting antenna size (Figure 2a). In contrast, under low-light-growth conditions, as occurs with high cell densities and with mutual self-shading, NAB1 repressor activity would be reduced and LRE–*CAO* mRNA translation would increase, resulting in greater Chl *b* levels and larger light-harvesting antenna size (Figure 1b). As a negative control to demonstrate that NAB1 levels indeed modulated the level of LRE–CAO translation, transgenic strains with a mutated LRE element (MUN) were produced in which the third base of each potential LRE amino acid codon was modified to not alter the LRE protein coding sequence but to disrupt the LRE consensus binding sequence that, in turn, prevents *CAO* translational modulation by NAB1. Finally, a positive control strain was generated in which the *cbs3* mutant (Comp-*cbs3-4*) was complemented with the wild-type *CAO* gene expressed under regulation of the strong *psaD* promoter/terminator.

Perrine *et al.* (2012) previously demonstrated that the rate of closure of PSII reaction centers as measured by Chl fluorescence rise kinetics was inversely correlated with the Chl *a/b* ratio or directly correlated with the light-harvesting antenna size. To determine the effects of NAB1 regulation on Chl *b* synthesis and on light-harvesting antenna size, rates of PSII closure in NC transgenics were compared with those of the *CAO* complemented *cbs3-4* lines and MUN lines following continuous growth in either low (subsaturating) or high (saturating) light environments (Perrine *et al.*, 2012) (Figure 2c). Reversible changes (*c.* 10%) in the rate of PSII closure (calculated at the time point when the Comp-*cbs3-4* line achieved 90% saturation based on Chl fluorescence raise kinetics) were observed upon transfer of NC cultures from low light to high light, high light to low light, and back again to high-light growth conditions. These results indicate that over the time period (24 h) of the change in growth light intensities the NC transgenics were capable of reversible alterations in the optical cross-section of their light-harvesting antenna size which is consistent with light regulation of Chl *b* accumulation. In contrast with the NC transgenics, the wild-type controls, the *CAO* complemented *cbs3-4* line, and the MUN lines had less than a 1–2% change in the rate of PSII closure following shifts to different growth light intensities (Figure 2c). Significantly, changes observed in antenna size in NC transgenics were reversible upon transfer of cultures from low light to high light and back to low light again; this indicates that antenna size regulation by NAB1 is highly dynamic. Three independent NC lines (NC-7, NC-29, NC-77) having the greatest range in alterations in Chl *a*/*b* ratios following shifts in growth light intensities were then selected for further detailed molecular, biochemical, and biophysical analyses to determine the impact of dynamic Chl *b* accumulation on photosynthesis and growth.

In contrast with wild-type cells, the *CAO* complemented *cbs3* mutant (Comp-*cbs3-4*), and the MUN lines, the Chl *a/b* ratios of the NC transgenics (NC-7, NC-29, NC-77) changed substantially (from 3 to 5.5) when grown at low versus high light intensities indicative of the ability of the NC transgenics to adjust their peripheral antenna sizes to different light intensities (see Figure 2d and Table 1). To determine whether antenna sizes and photosynthetic parameters continuously changed with increasing culture cell densities and self-shading, we compared Chl *a*/*b* ratios, photoautotrophic growth rates, and biomass accumulation of NC transgenic algae with those of wild-type algae. The environmental photobioreactors (ePBRs) used in this study (see Experimental procedures) have a light path of 20 cm similar to an algal production pond and further they were operated using a sinusoidal 12 h light–dark period reaching a peak light intensity at solar noon. As shown in Figure 3(a) (cf. Figure 3b; described later), the Chl *a*/*b* ratios of high-light-grown cells decreased from 4.2 to 3.1 for NC-77, from 3.7 to 2.9 for NC-7, and from 3.4 to 2.4 for the NC-29 line as the culture densities and self-shading increased. In contrast with the NC transgenics, the Chl *a*/*b* ratios (*c.* 2.5) of the parental wild-type strain (CC2677) and Comp-*cbs3-4* line did not change appreciably during the 12-day cultivation time period indicating that these strains have limited ability to adjust their light-harvesting antenna size as a function of light intensity or culture density. In addition, NC strains grown at lower light intensities had lower Chl *a*/*b* ratios consistent with dynamic light regulation of Chl *a*/*b* ratios (Figure 3b).

Interestingly, each of the NC lines had nearly identical rates of change in their Chl *a/b* ratios (*c.* Δ0.12/day) over time as well as nearly identical reductions in total Chl content per cell (*c.* 15% for NC lines) relative to wild-type *Chlamydomonas* as self-shading increased with culture age. These results suggest that LHCII and Chl partitioning between cells during and after chloroplast division was identical for the three independent NC transgenic lines.


*The Plant Journal*, (2020), doi: 10.1111/tpj.14751

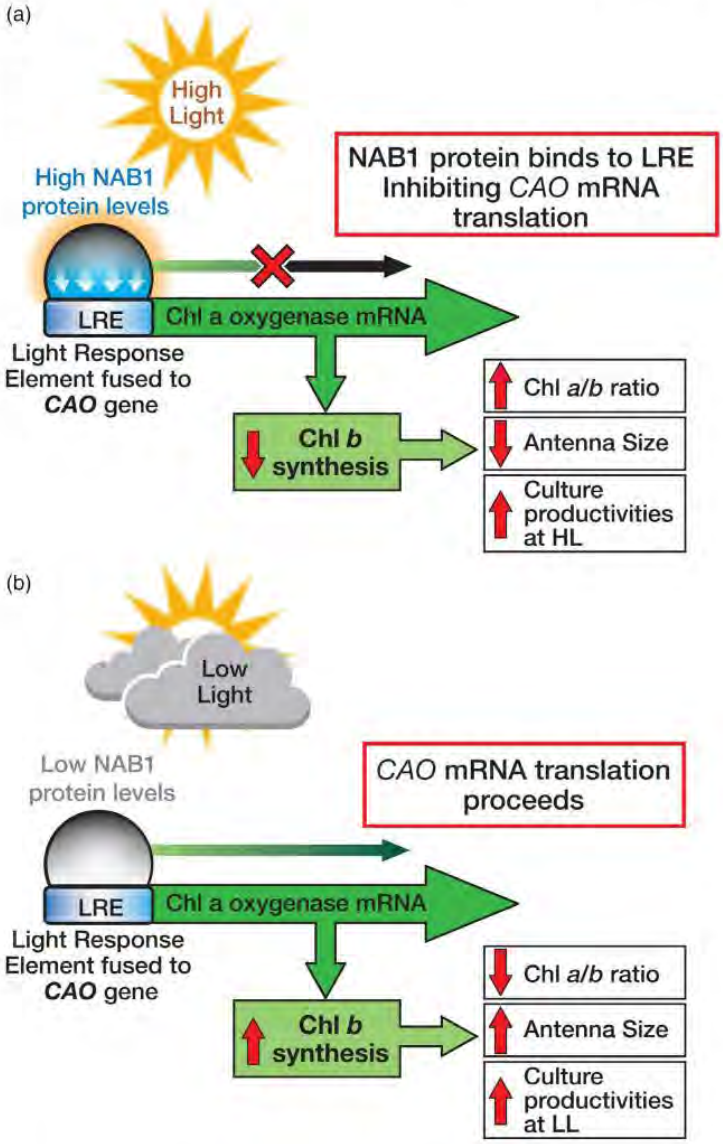


**Figure 1.** A model for NAB1 regulation of LRE–*CAO* expression in changing light environments. (a) At high light intensities, the NAB1 (Nucleic acid binding1) protein binds to light responsive element (LRE) fused to the 5′ end of the *CAO* (*Chlorophyllide a oxygenase*) transcript, inhibiting its translation and the synthesis of Chl *b*, resulting in a reduced PS II peripheral antenna size. (b) At low light intensities, NAB1 expression/activity is reduced allowing for *CAO* expression and enhanced Chl *b* synthesis resulting in an increase in PS II peripheral antenna size.

**Photosynthetic efficiency is higher in algae with self-adjusting antenna than in wild-type algae**

To assess the impact of the antenna alterations on photosynthetic rates, $CO_2$-dependent rates of oxygen evolution were measured in air and with saturating concentrations of bicarbonate at various light intensities. For this experiment, cells were harvested at the same culture age during mid-log phase. We note that these data represent only a snapshot of the impact of antenna size alterations on photosynthetic activity at a particular point in time generally determined when culture growth has the fastest (log phase) growth. When measured in air-saturated water, the NC lines had substantially greater photosynthetic rates than the wild-type, the *CAO* complemented *cbs3* mutant, and/or the *cbs3* mutant which had the lowest Chl content per cell. These results indicate that simple reduction in Chl content per cell is not associated with the highest photosynthetic rates (Figure 3c,d). At saturating light intensities, the NC-77 line had a photosynthetic rate that was 1.8-fold greater than in the CAO complemented *cbs3* mutant (Comp-*cbs3-4*) and 3-fold greater than in the parental


*The Plant Journal*, (2020), doi: 10.1111/tpj.14751

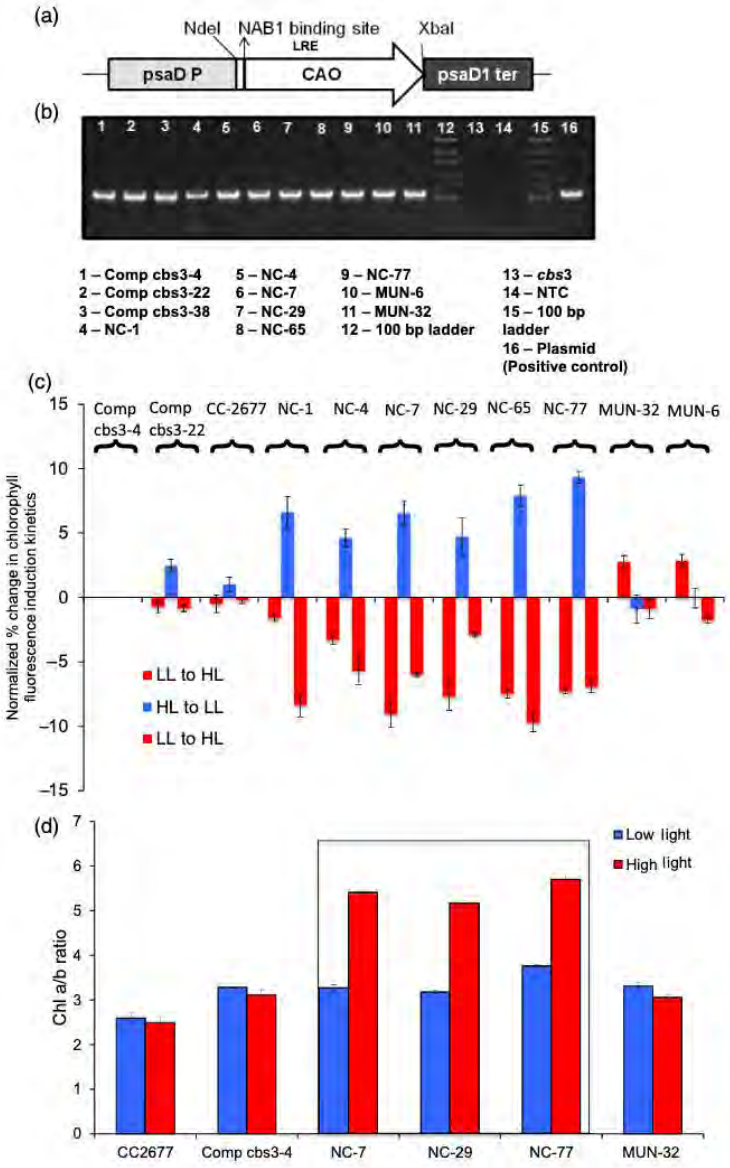


**Figure 2.** Selection of NAB1 transgenics. (a) A schematic representation of NAB1-CAO construct. The NAB1 binding site is introduced immediately downstream of the *CAO* start codon that is part of the Nde1 site. (b) PCR confirmation of the *Chlamydomonas* transgenics containing the *LRE–CAO* gene fusion. Comp *cbs3-4, 22,* and *38* are *cbs3* mutant complemented with CAO gene, NC 1, 4, 7, 29, 65 and 77 are NABCAO transgenics, MUN 6 and 32 represent mutated NAB1 transgenics. (c) Changes in chlorophyll fluorescence induction kinetics (related to antenna size) in the parental wild-type, and transgenic lines following acclimation to low (50 μmol photons $m^{-2}$ $sec^{-1}$) transfer to high (500 μmol photons $m^{-2}$ $sec^{-1}$) light and transfer back to low light. Data are the average and SD of three independent measurements. (d) Chl *a*/*b* ratios of wild-type and transgenic strains grown in shaker flasks at low (50 μmol photons $m^{-2}$ $sec^{-1}$) and high (500 μmol photons $m^{-2}$ $sec^{-1}$) light. Chl *a* and *b* content in cells was analyzed by HPLC. These results represent the average and ±SD of three to four independent biological replicates.

strain, CC2677. While photosynthesis was light saturated in the parental strain at around 600 μmol photons $m^{-2}$ $sec^{-1}$; it was not light saturated even at 800 μmol photons $m^{-2}$ $sec^{-1}$, in the NC-77 and NC-29 transgenics, presumably associated with the smaller antenna size (Figure 3c). Similar increases in photosynthetic rates for NC transgenics were also observed in the presence of saturating amounts of bicarbonate measured at maximum light intensities. The higher photosynthetic rates observed in NC transgenics in the presence of elevated $CO_2$ relative to air-saturated rates of photosynthesis indicates that other downstream limitations in photosynthesis associated with constraints in $CO_2$ assimilation and metabolism also impair overall photosynthetic efficiency and that additional improvement in photosynthetic efficiency could be achieved by enhancing carbon flux through the Calvin–Benson cycle (Figure 3d).

As photosynthetic rates are here expressed (Figure 3) based on Chl concentrations, we expect that the reductions in the Chl content per cell between transgenic and wild-type

**Table 1** Non-photochemical quenching, PSII photochemistry, and PSII functional antenna size of mid-log phase, high-light grown cells

| Traits | CC2677 | Comp-*cbs3-4* | *cbs3* | NC-7 | NC-29 | NC-77 |
|---|---|---|---|---|---|---|
| NPQ | 1.52 ± 0.12 (100%) | 1.21 ± 0.12 (80%) | 0.35 ± 0.06 (23%) | 1.17 ± 0.04 (77%) | 1.09 ± 0.01 (72%) | 1.05 ± 0.07 (69%) |
| Fv/Fm | 0.59 ± 0.04 (100%) | 0.62 ± 0.01 (105%) | 0.61 ± 0.05 (103%) | 0.57 ± 0.05 (97%) | 0.58 ± 0.01 (98%) | 0.65 ± 0.03 (110%) |
| $\sigma_{PSII}$ (Å$^2$) | 338 ± 50.2 (100%) | 372 ± 4.2 (110%) | 88 ± 14.8 (26%) | 287 ± 6.4 (85%) | 341 ± 51.6 (100%) | 263 ± 7.8 (78%) |

Algae were grown in flask cultures photoautotrophically for 4 days at a light intensity of 500 μmol photons m$^{-2}$ sec$^{-1}$. NPQ and the quantum efficiency of photosystem II ($F_v/F_m$) were measured using a FluoroCAM MF800. The functional absorption cross-section of PSII ($\sigma_{PSII}$) was measured using the FIRe instrument. Values present here are means ± SD, ($n$ = 3).

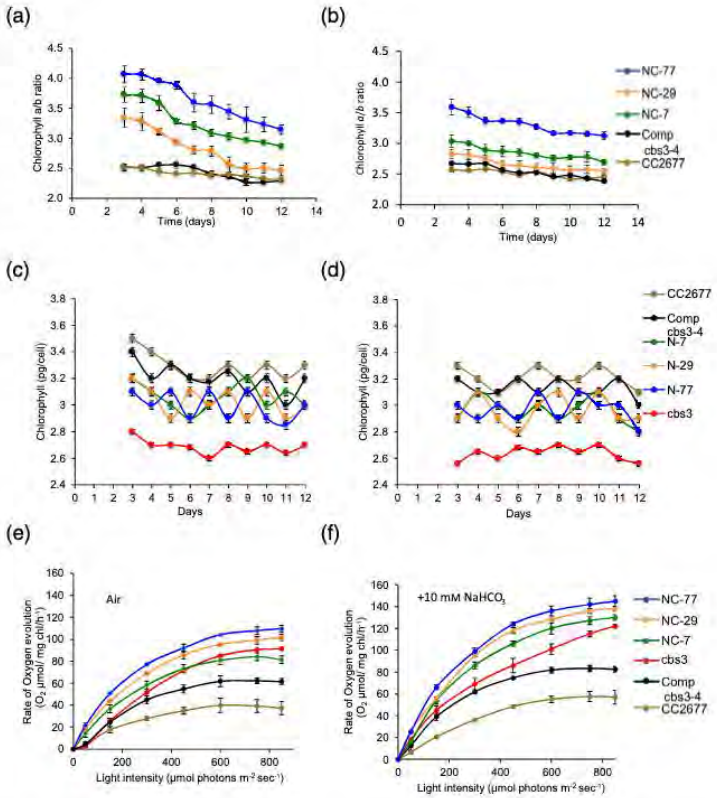


**Figure 3.** Chl *a*/*b* ratios and photosynthetic oxygen evolution, of NC transgenics (NC-7, NC-29 and NC-77), Chl *b* less (*cbs3*), the *CAO* complemented *cbs3* strain (Comp-*cbs3-4*), and its parental strain (CC2677). Change in Chl *a*/*b* ratio during growth in ePBR under a 12 h sinusoidal light–dark cycle with a peak photon flux at mid-day of: (a) 2000 μmol photons m$^{-2}$ sec$^{-1}$ (high light) or, (b) 300 μmol photons m$^{-2}$ sec$^{-1}$ (low light). Chl *a*/*b* ratios were measured from day 3 to day 12. (c) Chl content in 2000 μmol photons m$^{-2}$ sec$^{-1}$ (high light) grown cultures, (d) Chl content in 300 μmol photons m$^{-2}$ sec$^{-1}$ (low light) grown cultures. These data represent chlorophyll content per cell. Light-dependent rates of photosynthesis for log-phase cultures grown in low light (50 μmol photons m$^{-2}$ sec$^{-1}$). (e) Photosynthetic measurements made in air or, (f) in the presence of 10 mM $NaHCO_3$. Chl *a*/*b* ratios of the various strains at the time of photosynthetic measurements were: 2.45 ± 0.15 (CC2677), 2.49 ± 0.10 (Comp-cbs3-4), 2.99 ± 0.14 (NC-7), 3.15 ± 0.12 (NC-29), and 3.37 ± 0.11 (NC-77). All results represent the average and ±SD of three to four independent biological replicates.

strains would potentially bias measurements of photosynthetic rates. To determine if differential reductions in the Chl content/cell could account for the three-fold increase in photosynthetic rates (normalized on Chl content), we measured the Chl content per cell using light scattering ($OD_{750}$) as a proxy for cell number. We note that there is an identical linear correlation between $OD_{750}$ and the cell number for all strains except the *cbs3* mutant, which has the lowest Chl content per cell and the lowest photosynthetic performance (Figure S1). Overall, the Chl content/cell in the NC transgenics was 10–15% lower per cell relative to wild-type (Figure 3b). Importantly, we note that the *cbs3* mutant had that the greatest reduction in Chl content per cell also had the lowest photosynthetic rate per unit Chl. Thus, reduction in Chl/ cell could not solely account for the different photosynthetic rates observed between the various NC transgenics and the *cbs3* mutant. Finally, to determine if alterations in Chl *b* levels were associated with alterations in PSII activity, the PSII quantum efficiency was compared between the various strains. We observed that all the NC transgenic lines, used here, had near wild-type PSII quantum efficiencies except for NC-77 which had a 10% increase in PSII quantum efficiency relative to its parental wild-type line, consistent with its highest photosynthetic rates (Table 1).


*The Plant Journal*, (2020), doi: 10.1111/tpj.14751

**Susceptibility to photodamage increases with substantial reductions in light-harvesting antenna size**

There are multiple energy dissipation pathways by which excess energy is dissipated at high light intensities including heat (NPQ) and/or by generating damaging singlet oxygen species (Gilmore *et al.*, 1996a,b; Li *et al.*, 2009; Berman *et al.*, 2015). At saturating light intensities, NPQ is activated by increasing acidification of the thylakoid lumen associated with increased rates of proton-coupled electron transfer (Müller *et al.*, 2001). Excess Chl excited states are then dissipated as heat associated with electronic interactions between excited state Chls and xanthophyll cycle carotenoid(s) (Li *et al.*, 2009). Although the molecular mechanisms of NPQ in algae remain to be fully elucidated, several mechanisms have been proposed in land plants, including the formation of a charge transfer state between Chl *a* and zeaxanthin (Zx) in CP29 and its subsequent charge recombination (Holt *et al.*, 2005), and energy transfer from Chl *a* to lutein in LHCII and its subsequent thermal relaxation (Ruban *et al.*, 2007). Zx which accumulates under high light has also been proposed to induce reorganization of the PSII supercomplex, which can lead to aggregation of LHCII complexes and enhanced Chl-to-lutein energy transfer quenching (Johnson *et al.*, 2011). As shown in Table 1, the Chl *b*-less mutant, *cbs3*, had virtually no capacity to carry out NPQ as determined by Chl *a* fluorescence quenching in the presence of actinic light. In contrast, the NC transgenics had maximum NPQ levels that were similar to those of wild-type (Table 1).

To determine the molecular basis of antenna size modulation on NPQ, we compared the levels of photoprotective carotenoid pigments involved in NPQ from low- and high-light-grown strains. Alterations in the relative abundance of the major xanthophyll cycle pigments, Vx, Ax and Zx, are associated with alterations in NPQ (Havaux *et al.*, 2007; Wang *et al.*, 2008; Demmig-Adams *et al.*, 2016). Under high-light-growth conditions the steady-state levels of β-carotene and Vx were substantially (1.2–2-fold) reduced in NC transgenics, relative to low-light-grown cells, while photoprotective Zx levels were markedly increased (4.5–6-fold) suggesting an active xanthophyll cycle and NPQ in the NC transgenics (Figure 4d–f). Surprisingly, there was no increase in Zx content in the *cbs-3* mutant or its parental wild-type strain (Figure 4a, b). However, we observed a 1.5-fold increase in Zx in the *CAO* complemented *cbs-3* (Comp *cbs3-4*) transgenic line when grown under high light compared with the cells when grown under low light. Further, high-light-grown NC lines displayed up to a two-fold increase in the total de-epoxidation status (0.5 Ax + Zx/ Vx + Ax + Zx) of the xanthophylls compared with the Comp-*cbs3-4* transgenic and its parental wild-type strain (CC2677), clearly indicating more active NPQ in the NC transgenic strains (Figure 5a). These results suggest that increases in Zx were associated with elevated NPQ levels in *Chlamydomonas*. Similarly, lutein, another photoprotective pigment, accumulated to higher steady-state levels (1.5–2.2-fold) in the NC lines than in the wild-type (no change) or in the *cbs3* mutant where lutein levels actually decreased under high-light growth conditions. Collectively, the reduced ability to generate carotenoid species (Zx and luteain) that can quench Chl excited states in the *cbs3* mutant demonstrates that this NC parental strain has substantially impaired ability to carry out NPQ. In contrast, the increased ability of the NC transgenics to accumulate Zx under high light intensities, likely contributes to their improved photosynthetic performance in fluctuating light particularly relative to the *cbs3* mutant (Kromdijk *et al.*, 2016; Friedland *et al.*, 2019).

Multiple studies have implicated that the LHCSR3 protein is required for activating NPQ in green algae. The LHCSR3 protein has been shown to binds Chl *a* and *b*, Vx, lutein, and Zx (Li *et al.*, 2009; Peers *et al.*, 2009; Bonente *et al.*, 2011; Liguori *et al.*, 2013). In addition, it has been shown that LHCSR3 is associated with energy-dependent quenching (qE) in *Chlamydomonas* (Bonente *et al.*, 2011; Liguori *et al.*, 2013; Tokutsu and Minagawa, 2013). To assess the impact of antenna size modulation on LHCSR3 levels, we investigated the abundance of LHCSR3 in low-light- and high-light-grown cultures (Figure 5b). Consistent with the findings of Richard *et al.* (2000), low-light-grown wild-type cultures exhibited low LHCSR3 abundance. However, when wild-type cells were grown in high light, LHCSR3 levels were elevated. Under similar comparitive conditions, we observed elevated LHCSR3 levels in the Comp-*cbs3-4* transgenics and in two of the three NC transgenics (NC-29, and NC-7). Notably, the NC-77 transgenic, which had the smallest average antenna size of the three NC transgenics, had slightly lower amounts of LHCSR3 relative to the other NC lines (Figure 5b). It is apparent, however, that the lower LHCSR3 abundance (relative to wild-type) in the NC-77 line was sufficient to support high NPQ activity. In summary, we observed that NC lines had substantially higher steady-state levels of Zx, lower β-carotene, higher lutein levels, and in some cases elevated LHCSR3 levels than wild-type (CC2677) when grown in high light relative to low light (Figures 4d–f and 5a), demonstrating high NPQ activity in NC transgenics engineered to have adjustable light-harvesting antenna sizes.

**The capability for state transitions is not impaired by antenna size modulation**

The peripheral light-harvesting antenna protein complexes can also alter energy dissipation pathways by facilitating

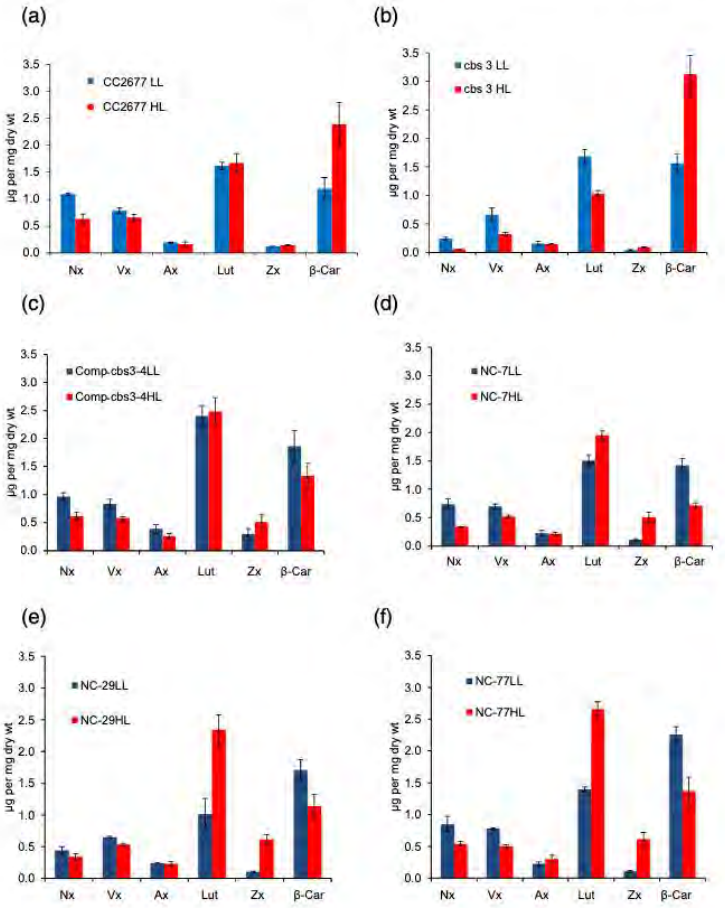


**Figure 4.** Carotenoid levels of low (LL:50 µmol photons $m^{-2}$ $sec^{-1}$) and high light (HL; 500 µmol photons $m^{-2}$ $sec^{-1}$) grown cells. Shaker flask grown algae cells were grown for 5 days and pigments (Nx, neoxanthin; Vx, violaxanthin; Ax, antheraxanthin; Lut, Lutein; Zx, zeaxanthin; and β-car, β-carotene) were analyzed by HPLC for: (a) CC2677 (wild-type *cbs3* parent), (b) *cbs3*, (c) Comp *cbs3*-4 (Comp-*cbs3*-4), (d) NC-7, (e) NC-29, and (f) NC-77. Results are the average and ±SD of three independent biological replicates.

the redistribution of energy between the two photosystems, particularly in algae. During high light exposure, certain members of the LHCII family are phosphorylated by a redox-regulated kinase that 'senses' the redox state of the PQ pool. Phosphorylation of LHCII and its subsequent migration between the two photosystems regulates energy distribution between photosystems (Wollman, 2001; Rochaix, 2007; Nagy *et al.*, 2014). This process is known as state transitions and is readily observed when algae are either pre-illuminated with light (≥715 nm) predominantly absorbed by PSI (State 1) or by light intensities that result in saturation of PSII electron transfer (State 2) (Takahashi *et al.*, 2006). As shown in Figure 6, we observed elevated and accelerated Chl fluorescence rise kinetics relative to dark-adapted cells in the wild-type, all NC transgenics, and the Comp-cbs3-4 lines following pre-illumination with PSI light. Significantly, the maximum level of Chl fluorescence induced in cells pre-illuminated with PSI-specific light was reduced in NC transgenics indicative of the capacity to carry out state transitions, unlike the *cbs3* mutants (Figure 6a–f). In summary, algae with self-adjusting antenna sizes (NC lines) were able to carry out active state transitions and NPQ unlike the *cbs3* mutant which has the smallest light harvesting antenna size and lacks Chl *b*.

### Self-adjusting antenna lines show reduction in LHC trimer levels associated with increasing Chl *a*/*b* ratios

To understand the effect of varying Chl *a/b* ratios on the relative qualitative abundance of specific thylakoid membrane LHC complexes and LHCII complex organization, we employed blue native gel electrophoresis (Järvi *et al.*, 2011). We grew NC transgenics, CC2677 (wild-type), Comp-cbs3-4 and the *cbs-3* strain in low-light and high-light conditions to assess the impact of growth light intensity and changes in Chl *b* levels on the relative abundance of major Chl–protein complexes (Kirst *et al.*, 2012; Friedland *et al.*, 2019).


*The Plant Journal*, (2020), doi: 10.1111/tpj.14751

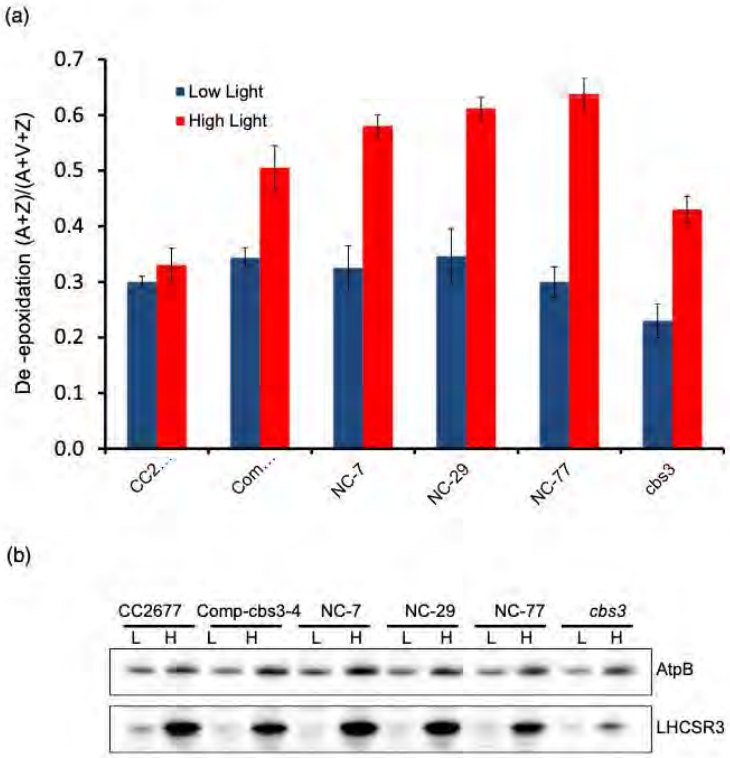


**Figure 5.** Photoprotective carotenoid de-epoxidation status and LHCSR3 expression of NC transformants, Chl *b* less (*cbs3*), *CAO* complemented *cbs3-4* (Comp-*cbs3-4*), and parental (CC-2677) strains. Cells were grown in shaker flasks in low light (50 μmol photons $m^{-2}$ $sec^{-1}$) for 7 days or in high light (500 μmol photons $m^{-2}$ $sec^{-1}$) for 4 days. (a) De-epoxidation (A + Z)/(A + Z + V) plotted for all the samples used; pigments were analyzed by HPLC as in Figure 3. Results are the average of three biological replications ±SD, and (b) LHCSR3 expression, as analyzed by SDS-PAGE and immunoblotting, and as described by Tokutsu and Minagawa (2013).

Wild-type, the Comp-*cbs3-4*, and NC transgenics all had similar apparent levels of the major PSI and PSII Chl–protein complexes (Figure 7). The NC transgenics, however, all had reduced LHCII trimer and monomer abundance relative to wild-type associated with their relative levels of Chl *b* reduction. These results were as expected, as the LHCII trimers have among the highest proportion of Chl *b* to Chl *a* of any of the peripheral light-harvesting proteins and, therefore, would presumably be the most sensitive Chl–protein complexes to reduction in Chl *b* levels (Table S1). A comparison of LHCII complex abundance (Figure 7a, b) between high-light- and low-light-grown wild-type (CC2677) and the Comp-cbs3-4 mutant showed very little difference in the antenna complex organization and abundance between low- and high-light-grown cells. This result is consistent with the lack in change of Chl *a/b* ratios observed in these strains when grown under these different light intensities (Figure 7a,b).

The apparent reduction of Chl *b* in LHCII trimers and monomers in the NC transgenics is also in agreement with our analysis of the functional cross-section ($\sigma_{PSII}$) of the PSII antenna. We observed a 20% reduction in the PSII antenna size in the NC transgenics and a 70% reduction in the *cbs-3* strain (Chl *b*-less mutant) (Table 1). Finally, in contrast to the NC transgenics, the *cbs-3* strain had only PSII dimer and PSII monomer complexes indicating that this strain is unable to form higher order complexes (PSII/PSI complex). Overall, these results suggest that LHCII trimers are most sensitive to reductions in Chl *b* content among all the LHC family members consistent with their high Chl *b* content (Ballottari *et al.*, 2009; Natali and Croce, 2015).

### Antenna modulation changes the thylakoid membrane structure in self-adjusting antenna lines

Any reduction in Chl–protein complexes would also be expected to impact protein–lipid packing in thylakoid membranes and stacking as well as spacing interactions between thylakoids (Mussgnug *et al.*, 2007; Friedland *et al.*, 2019). To determine if dynamic antenna size modifications had any impact on thylakoid membrane structure and stacking, we assessed changes in membrane architecture (Figures 8, S2 and S3) in wild-type, the *cbs-3* mutant as well as the NC transgenic lines. We observed that both thylakoid membrane packing and the lumen space was greater in the NC transgenics than in the wild-type cells (Figure 8). The NC transgenics had 11–20% thicker

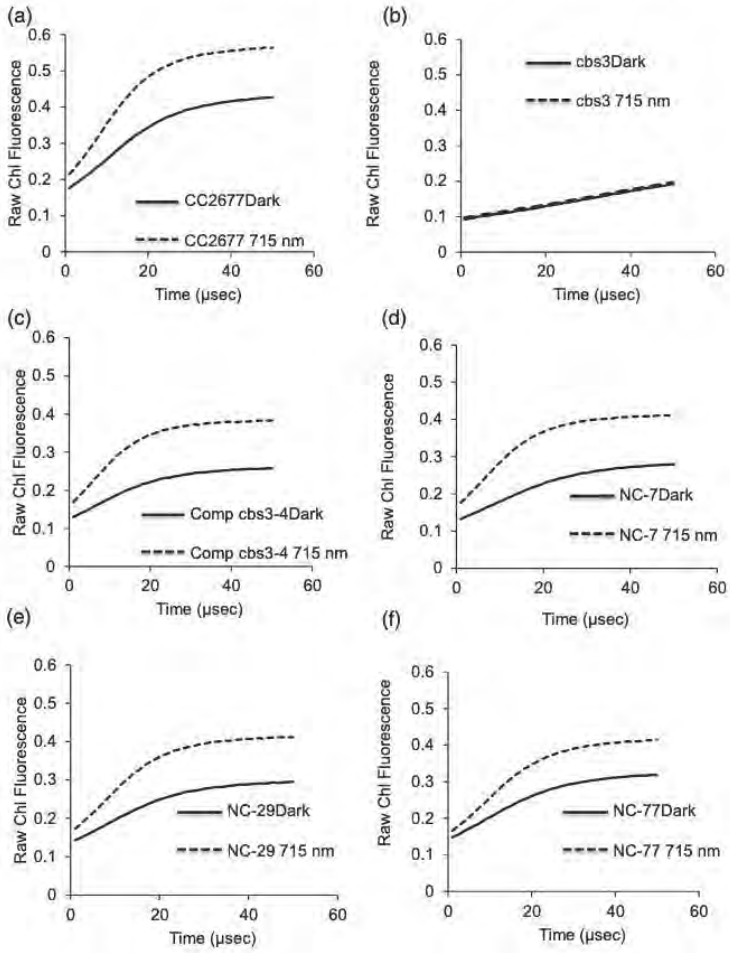


**Figure 6(a–f).** Chlorophyll *a* fluorescence transients after dark adaptation or following pre-exposure to 715 nm (PSI) light for low-light-grown (50 μmol photons $m^{-2}$ $sec^{-1}$) NC transformants, Chl *b* less (*cbs3*), *CAO* complemented *cbs3-4* (Comp-cbs3-4) and parental strain (CC2677). Chl fluorescence was measured under continuous, non-saturating illumination.

thylakoid membranes compared with wild-type and the Comp *cbs3-4* strain, while the Chl *b*-less *cbs-3* mutant had substantially reduced membrane thickness (Figure 8g). We also observed a 10–16% increase in lumen space in the NC lines compared with the wild-type and the Comp *cbs3-4* strains, and up to a 33–41% increase compared with the *cbs-3* mutant (Figure 8h). One of the very striking differences in membrane architecture observed in the NC transgenics was the reduction in the number of thylakoids in each stack. Whereas, the wild-type and the Comp *cbs*3-4 lines had on average 10–12 thylakoid per stack, the NC transgenics had only 2–6 thylakoids per stack associated with greater stromal surface area (Figure 8a–f). These results are consistent with earlier studies that had demonstrated that modulation in antenna protein levels is associated with alterations in thylakoid membrane structure and stacking (Mussgnug, 2005; Mussgnug *et al.*, 2007; Friedland *et al.*, 2019).

**NC transgenics with self-adjusting antenna accumulate substantially more biomass compared with wild-type**

Finally, we assessed whether the capability to dynamically alter antenna size and photosynthetic rates as a function of growth light-intensity impacted biomass yield. As shown in Figure 9(a), NC transgenics, having initial Chl *a/b* ratios close to 5 (low cell density growth conditions), had the highest initial growth rates when grown under high light conditions (Figure 9c,d). The intrinsic (log) growth rate of the NC-77 line was 3.5-fold greater than that of the wild-type strain. However, all the wild-type and the transgenic strains had slower, and much more linear growth rates when grown at lower, subsaturating light intensities (Figure 9b). As expected, the Chl *a/b* ratios of NC lines grown at low light intensities were reduced relative to those of wild-type cells grown at high light intensities during their initial growth (low cell density) phases. Significantly,


*The Plant Journal*, (2020), doi: 10.1111/tpj.14751

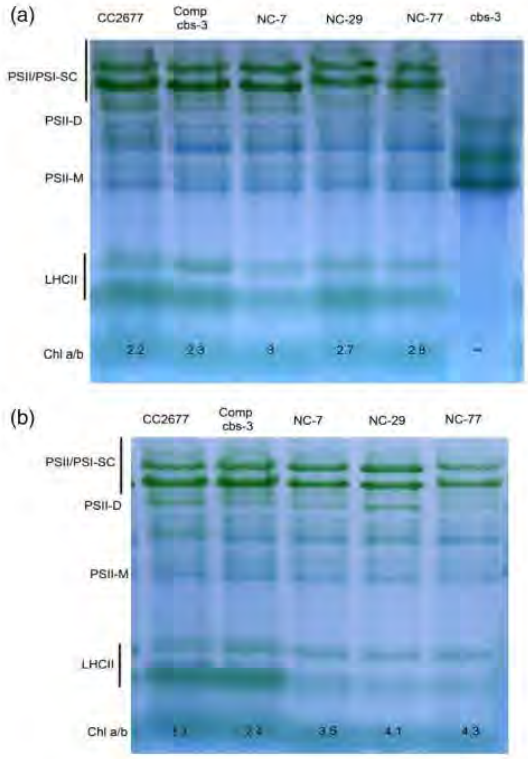


**Figure 7.** Blue native-PAGE (BN-PAGE) analyses of thylakoid membrane protein complexes. Thylakoid membranes were isolated from low-light- and high-light-grown cultures of wild-type CC2677, NC lines, Comp-cbs3-4 and cbs-3 strain and subjected to BN-PAGE. Identification of the thylakoid membrane protein complexes was carried according to Kirst *et al.* (2012). PSII–LHCII complex and PSI–LHCI complex; PSII-D, PSII dimer; PSII-M, PSII monomer; LHCII, Chl *a*/*b* light-harvesting complex are indicated in the figure. (a) BN-PAGE protein–Chl complexes for low light (50 μmol photons $m^{-2}$ $sec^{-1}$) grown cells. (b) BN-PAGE protein–Chl complexes for high light (500 μmol photons $m^{-2}$ $sec^{-1}$) grown cells.

biomass yields of the NC lines were 1.8 to 3-fold greater than the wild-type lines at both low and high light growth conditions (Figure 9c,d). The fact that NC transgenics had similar biomass yields when grown at low or high growth light intensities demonstrates that the ability to carry out light-intensity dependent adjustments in antenna size can, enhance biomass yields under a variety of light conditions.

## DISCUSSION

Earlier studies have shown that a slight reduction in the size of the peripheral light-harvesting antenna in green algae and plants, leads to enhanced photosynthetic rates, greater high-light photoprotection, and substantial increases in biomass productivity (Perrine *et al.*, 2012; Friedland *et al.*, 2019). This smaller and more efficient antenna size corresponded to the loss of one LHCII trimer associated with a partial reduction in Chl *b* levels (Chl *a*/*b* ratio of 5). These small reductions in light-harvesting antenna size were also shown to allow deeper penetration of photosynthetically active radiation into the algal culture or plant canopy allowing for greater rates of photosynthesis throughout the light column (Polle *et al.*, 2000; Mussgnug *et al.*, 2007; Stephenson *et al.*, 2010; Ort *et al.*, 2011; Mitra *et al.*, 2012; Perrine *et al.*, 2012; Subramanian *et al.*, 2013; Cazzaniga *et al.*, 2014; Friedland *et al.*, 2019). However, light intensities in algal ponds continuously change with time and depth as culture densities change. Thus, we suggested that further improvements in photosynthetic efficiency could be achieved by dynamically regulating light-harvesting antenna size to respond to continously changing light environments. By regulating Chl *b* synthesis in a light-dependent manner, we have demonstrated that the abundance of specific peripheral light-harvesting protein–Chl complexes and the optical cross section of the light harvesting antenna can be dynamically regulated as culture density and self-shading increases (Figure 3a,b). The generation of continuously adjusting light harvesting antenna sizes was acheived by light-regulated translational repression (Nab1) of a modified *CAO* gene. Significantly, not all transgenics with self-adjusting antenna sizes had similar photosynthetic rates at a given light intensity even though they had similar total Chl content per cell, indicating that even small differences in Chl *b* levels or peripheral antenna size, but not Chl content per cell, can have significant effects on photosynthetic efficiency (Figure 3e,f). Finally, consistent with earlier observations, we show that NC transgenics with self-adjusting antenna sizes having initial Chl *a*/*b* ratios near 5 had greater photosynthetic rates and biomass production than NC transgenics having Chl *a*/*b* ratios more similar to wild-type algae (Figure 9a, b) (Perrine *et al.*, 2012; Friedland *et al.*, 2019).

At the protein–Chl complex structural level, we observed that the primary effect of moderate reductions in Chl *b* levels (Chl *a*/*b* ratio, near 5) was a reduction in LHCII trimer complex abundance. This result is as expected since the trimeric LHCIIs have among the lowest Chl *a*/*b* ratios or the highest Chl *b* content (Table S1) of all the peripheral light-harvesting complex members, and thus is most likely to be reduced in protein abundance in association with a reduction in Chl *b* levels (Formaggio *et al.*, 2001; Friedland *et al.*, 2019). One potential consequence of the loss of loosely bound LHCII trimers is that the efficiency of excitation energy transfer between the more proximal CP29 and CP26 light-harvesting antenna complexes and the PSII reaction center antenna proteins (CP43 and CP47) would increase as energy transfer efficiency is greater between the CP29 and CP26 antenna complexes and the PSII reaction center antenna (CP43 and CP47) than between LHCII trimers and the CP29 and CP26 light harvesting antenna proteins (Drop *et al.*, 2014; Su *et al.*, 2019). This enhanced energy transfer efficiency from the proximal

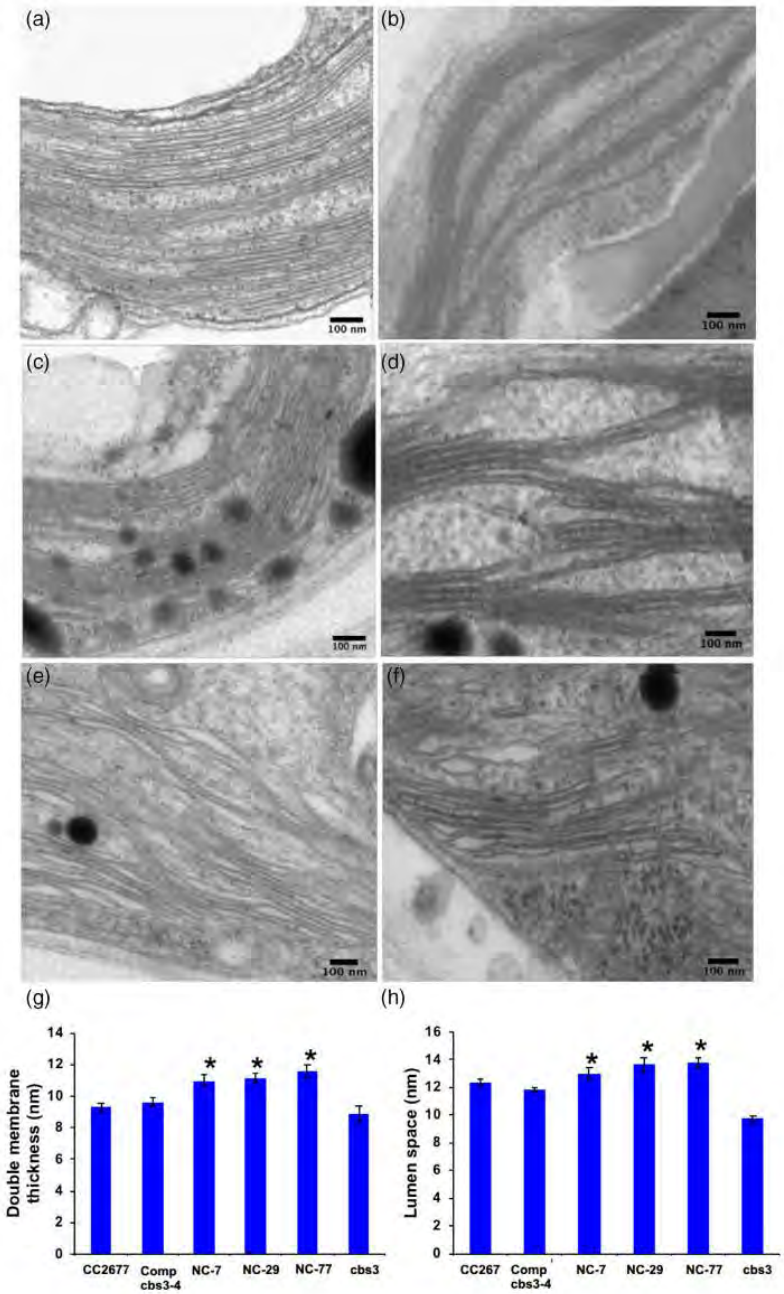


**Figure 8.** Transmission electron micrographs showing thylakoid membrane stacking and structure in wild-type CC2677 (a), cbs-3 (b), Comp *cbs3-4* (c), NC-7 (d), NC-29 (e), and NC-77 (f). These lines were grown under low light conditions. Scale bar represents 100 nm in all the TEM micrographs. Measurements for thylakoid membrane bilayer (g) and lumenal space (h) are also shown. These data represent the average ± SD of 150–200 measurements. The asterisk (*) indicates statistically significant differences between parental wild-type (CC2677) and NC transgenics, as determined by Student's *t*-test, with $P < 0.005$.

antenna to the reaction center antenna is presumably due to the greater distances between the LHCII trimers and the proximal antenna complexes than between the proximal antenna complexes and the PSII reaction center (Drop *et al.*, 2014). The net result of LHCII trimer loss is that the excitation energy transfer efficiency from the remaining


*The Plant Journal*, (2020), doi: 10.1111/tpj.14751

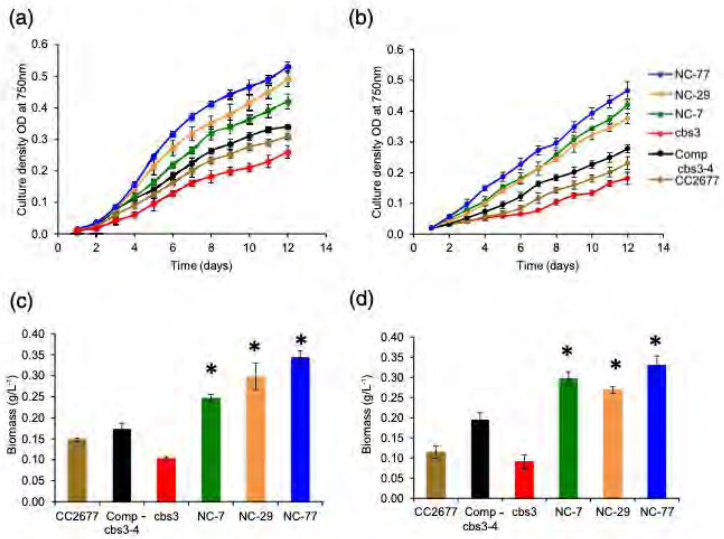


**Figure 9.** Photoautotrophic growth curves under a 12 h sinusoidal light–dark cycle with a peak photon flux at mid-day of; (a) 2000 μmol photons $m^{-2}$ $sec^{-1}$ (high light), or (b) 300 μmol photons $m^{-2}$ $sec^{-1}$ (low light). Dry cell biomass of cells after 12 days of growth in the environmental photobioreactor (ePBR) at mid-day of (c) 2000 μmol photons $m^{-2}$ $sec^{-1}$ (high light), or (d) 300 μmol photons $m^{-2}$ $sec^{-1}$ (low light). All results represent the average and ±SD of three to four independent biological replicates. The asterisk (*) indicates statistically significant differences in growth between parent wild-type and NC transgenics, determined by Student's *t*-test, with $P < 0.005$.

peripheral light harvesting complexes to the PSII reaction center complex should increase relative to that in the wild-type photosynthetic systems.

The partial reduction in LHCII trimer complexes may also impact downstream electron transfer processes. LHCII proteins play a key role in thylakoid membrane structural organization as well as in its stacking (Barber and Chow, 1979; Allen and Forsberg, 2001; Chow *et al.*, 2005). Mussgnug and co-workers showed that the *stm3* and *stm3LR3* mutants which have substantially reduced LHCII levels also had substantial alterations in thylakoid membrane packing and lumen spacing compared with wild-type parental strains (Mussgnug, 2005; Mussgnug *et al.*, 2007) Similarly, *tla1* mutants exhibited substantial alterations in thylakoid membrane organization and in the lumen space associated with losses in light-harvesting complexes similar to the *cbs3* Chl *b*-less line used in these studies (Mitra *et al.*, 2012).

Protein diffusion and mobility play a key role in photosynthetic efficiency as they can affect light-harvesting and electron-transport efficiency as well as the turnover and repair of the photosynthetic complexes (Kirchhoff *et al.*, 2004, 2008, 2013; Kirchhoff, 2014). Macromolecular crowding of membranes by protein complexes is known to affect the trafficking the two mobile electron carriers (plastoquinone and plastocyanin), which link the photosynthetic complexes I and II (Mullineaux, 2005, 2008; Kirchhoff *et al.*, 2008). Rates of the intersystem electron transport are also impacted by the rate of PQ shuttling between PSII and Cyt $b_6f$ complexes (Haehnel, 1984). In addition, the lateral diffusion of $PQH_2$ from PSII to the Cyt $b_6f$ complexes can be restricted by overcrowded lipid domains of thylakoid membranes. Thus, increases in thylakoid lumenal space and membrane thickness associated with reductions in the LHCII content in NC77 transgenics may further increase the rates of electron transfer by enhancing the diffusion rates of mobile electron carriers (Tremmel *et al.*, 2003; Chow *et al.*, 2005; Kargul *et al.*, 2005; Takahashi *et al.*, 2006; Kargul and Barber, 2008; Kirchhoff *et al.*, 2008; Kirchhoff *et al.*, 2013).

Based on previous studies in algae and plants having partially reduced Chl *b* levels several authors anticipated that alterations in light-harvesting Chl–protein abundance may have impacts on other photosynthetic functions such as NPQ (Perrine *et al.*, 2012; Friedland *et al*, 2019). Under high-light stress conditions, an increase in the accumulation of Zx is expected to reduce high-light-dependent photodamage such as the production of reactive oxygen species or lipid peroxidation. This is achieved by Zx quenching excess Chl excited states under high light (Li *et al.*, 2009). Significantly, Zx has been shown to provide photoprotection in the absence of LHCII, although to lesser degree than in the presence of LHCII (Havaux *et al.*, 2007; Dall'Osto *et al.*, 2010). Lutein has also been shown to provide protection against excited state Chl mediated photodamage (Ruban *et al.*, 2007; Li *et al.*, 2009). NC transgenics grown at high light intensities exhibited increased accumulation of the photoprotective pigments Zx and lutein compared with the wild-type, Comp *cbs3-4*, and *cbs-3* lines (Figure 4). In land plants, higher carotenoid levels and enhanced cycling of lutein and Zx have been correlated with greater recovery of photosynthetic rates following photoinhibition and associated with up to 15% increases in biomass accumulation in plants grown in the field (Long *et al.*, 1994; Wang *et al.*, 2002; Kromdijk *et al.*, 2016). Thus, improved photosynthetic performance in the NC

transgenics is established not only through antenna size modulation, but also through enhanced active photoprotective mechanisms (Friedland *et al.*, 2019). The net outcome is that antenna size reduction can have multiple pleiotropic effects that collectively enhance photosynthetic performance and stress tolerance through processes not anticipated by simple reductions in light harvesting optical cross section alone.

The important question is: Do the complex changes resulting from antenna size modulation impact biomass production? Previously, Perrine *et al.* (2012) observed a 40% increase in biomass yield in *Chlamydomonas CAO* RNAi lines having optimal Chl *a/b* ratios of 5. The NC-77 transgenic line, however, had a three-fold increase in biomass yield compared with wild-type. This increased biomass production in NC transgenics with adjustable light harvesting antenna sizes, however, raises the question why have algae and plants evolved large, less efficient, fixed light-harvesting antenna systems that oversaturate downstream electron transfer processes during most (80%) of the day. In mixed species environments, the ability to shade or reduce the light available to competing species may offer a selective advantage, because limiting light availability to other species would reduce their growth rates and presumably their fitness (Zhu *et al.*, 2008; Ort *et al.*, 2015). Species competing for light are clearly impacted by shading as plant canopies close or as algal cultures reach high cell densities. Thus, having large light-harvesting antenna systems may reduce light availability for competitors and enhance fitness for plants or algae that shade competitors as is the case in high-density algal cultures. In addition, plants living lower in the canopy or algae growing deeper in the water column often experience very low light conditions. Having a large light-harvesting antenna would allow photosynthesis and growth at light intensities that could not support the growth of algae with smaller antenna sizes optimized for growth at higher light intensities. In fact, algae that grow at extreme depths in the oceans have among the largest light-harvesting antenna sizes known in photosynthetic organisms (Yamazaki *et al.*, 2005).

In summary, we have demonstrated that light-regulated, translational modulation of *CAO* expression and Chl *b* accumulation is an effective means to dynamically regulate light-harvesting antenna size under fluctuating light environments. NC transgenic algae having initially optimized intermediate antenna sizes (Chl *a/b* ratio *c.* 5) yielded as much as three-fold more biomass than the wild-type algae. Light-harvesting antenna sizes associated with the maximum photosynthetic rates were associated with multiple traits that enhance photosynthetic efficiency including much more robust NPQ processes, and state transitions. Notably, the biomass accumulation rates observed in NC lines grown under field-like conditions meet the biomass productivity requirements identified in recent life-cycle analysis required to meet algal biofuel price points that are competitive with petroleum (Olivares *et al.*, 2016). Finally, these results have clear implications for the design of light-harvesting antenna systems in plant canopies for enhanced crop yields (Friedland *et al.*, 2019). Engineering plants or algae to be able to adjust their light-harvesting antenna size continuously to maximize light utilization efficiency can lead to substantial improvements in photosynthetic rates and biomass accumulation.

## EXPERIMENTAL PROCEDURES

### Growth conditions

*Chlamydomonas reinhardtii* Chl *b*-less mutant (*cbs3*) strain and its wild-type parental strain (CC2677) were obtained from Ayumi Tanaka and the *Chlamydomonas* Genetic Center, respectively (Tanaka *et al.*, 1998). Small cultures were grown at 25°C in 250 ml Erlenmeyer flasks containing 100 ml of a high salt (HS) medium and shaken at 150 rpm (http://www.chlamy.org/media.html). Cultures were inoculated from a log-phase culture, using 1 ml (1% volume) of cells. Flasks cultures were illuminated using fluorescent light at the light intensities indicated below.

### Generation of transgenic lines

For the generation of transgenic *Chlamydomonas reinhardtii cbs3* mutants, containing the NAB1 (Nucleic Acid Binding1) regulated LRE–*CAO* gene fusion, the LRE element was introduced into the 5′ end of the *CAO* gene by PCR using *Chlamydomonas* nuclear DNA as the template and the following forward, (ATCTTCATATGGGCCAGACCCCCGCAGGGCTTCCTGCGTCGCTTCAACGCAAGG) and reverse (TAGAATCTAGACTAGTTGTCCATGTCATCCTCGTCCACCGAG) primers. The LRE, NAB1-binding domain sequence (underlined) was included in the forward primer. The LRE encodes five additional amino acids, GQTPA, following the start methionine. The LRE–*CAO* PCR product was cloned into the PSL18 (Depège *et al.*, 2003; Mussgnug, 2005) nuclear expression vector using the *Nde*I and *Xba*I restriction sites downstream of the *PSAD* promoter (Kumar *et al.*, 2013). The plasmid carrying the LRE–*CAO* fusion gene was transformed into the *CAO* knockout strain *cbs3* (Tanaka *et al.*, 1998) by particle gun bombardment using the PDS-1000/He system (Bio-Rad, Richmond, CA, USA) (Kindle *et al.*, 1989). The bombarded cells were re-suspended and shaken overnight in liquid Tris acetate phosphate (TAP) medium and spread onto TAP-agar plates containing 50 μg $ml^{-1}$ ampicillin and 25 μg $ml^{-1}$ paromomycin for selection of transgenics. The PSL18 vector contains the *AphVIII* gene (Sizova *et al.*, 2001) driven by the *PSAD* promoter and terminator encoding paromomycin resistance. After 14 days, paromomycin-resistant algal colonies were transferred to fresh TAP-agar plates containing 50 μg $ml^{-1}$ paromomycin. The transformants were designated as NC (NAB CAO). Multiple transgenics were screened for variations in Chl *a/b* ratios with changing light intensities. Three independent NC transgenic lines representative of the highest, mid and lowest Chl *a/b* ratios were selected for subsequent studies.

For the generation of the *CAO* complemented *cbs3* strain, the *CAO* gene was amplified by PCR using nuclear DNA from *Chlamydomonas* as the template and the following forward (ATCTTCA TATGCTTCCTGCGTCGCTTCAAC) and reverse (TAGAATCTAGAC TAGTTGTCCATGTCATCCTCGTCCACCGAG) PCR primers. The *CAO* gene was cloned into the PSL18 vector using the *Nde*I and


*The Plant Journal*, (2020), doi: 10.1111/tpj.14751

*Xba*I restriction sites and the resulting plasmid was transformed into the *cbs3* host strain, as described above. The transformants were designated as Comp-*cbs3-4*. Multiple transgenic lines were generated having similar Chl *a/b* ratios. One Comp-*cbs3-4* line was used for further analysis.

For the generation of the mutated *LRE–CAO* gene fusion (MUN), the *CAO* gene was amplified by PCR using the following forward (ATCTTCATATGGGGCAAACACCGGCGGGCCTTCCTGCGTCGCTT CAACGCAAGG) and reverse (TAGAATCTAGACTAGTTGTCCATGT CATCCTCGTCCACCGAG) PCR primers, respectively. The underlined sequence encodes the same N-terminal five amino acid insertion sequence (GQTPA) as the conserved LRE protein coding element but has four nucleotide substitutions at the codon wobble positions corresponding to bases 2, 5, 8, and 11 of the underlined sequence to alter the conserved LRE binding site. Thus, the only difference between the un-mutated and mutated *LRE–CAO* gene fusions is the LRE nucleotide sequence in the transgenic line (MUN). The PCR product was cloned into the PSL18 vector using the *Nde*I and *Xba*I restriction sites and transformed into the *cbs3* host strain, as described above. The transformants were designated as MUN. Three independent MUN transgenics were generated and the strain having the highest photosynthetic rate was analyzed further.

To confirm the presence of the *CAO* transgene in the transformed cells, total DNA was extracted from the transgenics, using the Chelex-100 extraction method (Cao *et al.*, 2009). Briefly, a small loop of cells was boiled in 50 μl of a 5% (w/v) solution of Chelex-100 resin (Bio-Rad) for 10 min. The mixture was briefly vortexed and spun down for 2 min in a microfuge at maximum speed to pellet the cell debris. The supernatant containing the transgenic DNA was used as the template for PCR. The presence of the transgene was confirmed by PCR using forward (GTTAGGTGTTGCGCTCTTGAC) and reverse (GGCGAGTGAGCA TATTCGTCC) primers, which hybridize to the *PsaD* promoter and the *CAO* gene, respectively.

### Photoautotrophic growth measurements and biomass estimation

Photoautotrophic growth of the wild-type (CC2677), *cbs3, CAO* complemented *cbs3-4* (Comp-cbs3-4), and the *LRE–CAO* gene fusion transformants; NC-7, NC-29, and NC-77 strains was measured using environmental photobioreactors (ePBRs; Phenometrics, San Diego, CA, USA) containing 500 ml of liquid HS media. All experiments were done in triplicates for each time point and each treatment. Light intensity was programmed for a 12 h sinusoidal light period with a peak mid-day intensity of 2000 μmol photons $m^{-2}$ $sec^{-1}$ (for high light) and 300 μmol photons $m^{-2}$ $sec^{-1}$ (for low light). The temperature was kept constant at 25°C, and the ePBRs were stirred with a magnetic stir bar at 200 rpm. Filtered air was bubbled constantly through the growing cultures. The optical density of the cultures was monitored on a daily basis at 750 nm, using a Cary 300 Bio UV–Vis spectrophotometer (Agilent, Santa Clara, CA, USA). After completion of any growth measurement, the total biomass content of the individual ePBR was harvested by centrifugation at 11 000 rpm for 15 min. Cell pellets were frozen immediately in liquid $N_2$ and later freeze dried, using a Microprocessor Controlled Lyophilizer (Flexi-Dry) for determination of total biomass.

### Chlorophyll fluorescence measurements

For Chl fluorescence induction analyses, cell suspensions of the parental wild-type and transgenic *Chlamydomonas* strains were adjusted to a Chl concentration of *c.* 2.5 μg $ml^{-1}$. Chl fluorescence induction was measured using the FL-3500 fluorometer (Photon System Instruments, Drasov, Czech Republic) (Nedbal *et al.*, 1999). The cells were dark adapted for 10 min before the measurement. Chl fluorescence was induced using continuous actinic illumination of 100 μsec duration and Chl fluorescence levels were measured every 1 μsec using a weak pulse-modulated measuring flash. The values of Chl fluorescence were normalized to the maximum achieved for a given sample. To identify transgenics that could reversibly adjust their light-harvesting antenna sizes in response to different growth light intensities, we measured the percentage light saturation of PSII activity at the time point when Comp-*cbs3-4* achieved 90% saturation of Chl Fmax (where Fmax is maximum Chl fluorescence in the dark-adapted state) following growth and transfer of the transgenics and control strains from low to high light, high light to low light, and low light to high light again for 1 day each (Figure 2b). Antenna size adjustment was expressed as a percentage change in Chl fluorescence yield relative to low-light-grown cells at the time point when the control (Comp-cbs4-4) achieved 90% of Fmax. For the state transition experiments associated with the migration of light-harvesting complexes between the photosystems, low-light-grown cultures were either dark adapted or pre-illuminated with 715 nm light for 10 min before the induction of Chl fluorescence. The actinic flash duration for this experiment was set to 50 μsec duration and Chl fluorescence was measured every μsec (Perrine *et al.*, 2012).

NPQ of the Chl excited state was determined using a FluorCam 800MF from Photon Systems Instruments. Algal cultures were photoautotrophically grown, in flasks, for 4 days in high light (500 μmol photons $m^{-2}$ $sec^{-1}$). The cells were pre-illuminated with weak far-red (730 nm) light (*c.* 5 μmol photons $m^{-2}$ $sec^{-1}$) for 30 min before fluorescence quenching analysis. Actinic light intensity was 750 μmol photons $m^{-2}$ $sec^{-1}$ and a saturation pulse was given at 3000 μmol photons $m^{-2}$ $sec^{-1}$. The NPQ of Chl fluorescence was calculated as $(F_m - F_m')/F_m'$, where $F_m$ is maximum fluorescence in dark-adapted state, and $F_m'$ is maximum fluorescence in light ($F_m'$ was measured using a series of saturating light pulses). PSII quantum yield was calculated as $(F_m - F_o)/F_m$, where $F_o$ is the minimum fluorescence. The absorption cross-section of PSII ($\sigma_{PSII}$) that reflects the functional antenna size of PSII was measured using a chlorophyll fluorescence induction and relaxation (FIRe) fluorometer system (Model FIRe, Satlantic, Nova Scotia, Canada) as described by Tokutsu *et al.* (2009).

### Photosynthetic oxygen evolution

$CO_2$-dependent rates of oxygen evolution were measured for low light (50 μmol photons $m^{-2}$ $sec^{-1}$) HS grown log-phase cultures (0.4–0.6 for OD at 750 nm) using a Clark-type oxygen electrode (Hansatech Instruments, Norfolk, UK). Cells were re-suspended in 20 mM HEPES buffer (pH 7.4) and air-saturated rates of oxygen evolution were measured, using 650 nm light of different intensities: 50, 150, 300, 450, 600, 750 and 850 μmol photons $m^{-2}$ $sec^{-1}$. This experiment was then repeated in the presence of 10 mM $NaHCO_3$. Photosynthetic light saturation curves were normalized on the basis of Chl as well as cell density ($OD_{750\ nm}$) (Perrine *et al.*, 2012). Chl levels were determined by the method described by Arnon (1949).

### Pigment analysis by high performance liquid chromatography (HPLC)

*Chlamydomonas* cultures were grown at low-light (50 μmol photons $m^{-2}$ $sec^{-1}$) and high-light (500 μmol photons $m^{-2}$ $sec^{-1}$) intensities for 5 days in HS media in shaker flasks. Cells were centrifuged at 3000 rpm for 3 min and immediately frozen in liquid nitrogen (77K) and lyophilized. Carotenoids and Chls were

extracted with 100% acetone in the dark for 20 min. After incubation, samples were centrifuged at 14 000 rpm for 2 min in a microfuge and the supernatant was transferred to a glass tube and dried under vacuum. The dried samples were re-suspended in 1 ml of acetonitrile: water: triethylamine (900:99:1, v/v/v) for HPLC analysis. Pigment separation and chromatographic analysis were performed on a Beckman HPLC equipped with a UV–vis light detector, using a C18 reverse phase column at a flow rate of 1.5 ml $min^{-1}$. Mobile phases were (A) acetonitrile/$H_2O$/triethylamine (900:99:1, v/v/v) and (B) ethyl acetate. Pigment measurement was carried out at 445 nm with reference wavelength at 550 nm (Tian and DellaPenna, 2001). Individual algal pigments were identified on the basis of their retention times and optical absorbance properties and quantified on the basis of their integrated absorbance peaks relative to known carotenoid standards. Carotenoid standards were purchased from DHI group, Denmark. Pigments were standardized on the basis of dry weight of three replicates.

### Thylakoid membrane isolation and blue native gel electrophoresis

The wild-type parent CC2677, Comp-cbs3-4, NC lines and the cbs-3 strain were all grown in 100–200 ml of liquid HS medium under low light intensity (50 μmol photons $m^{-2}$ $sec^{-1}$) or high light intensity (500 μmol photons $m^{-2}$ $sec^{-1}$) with continuous shaking at 225 rpm for 3 days. Cells were harvested by centrifugation at 3000 ***g*** for 5 min to obtain cell pellets. The cell pellet was re-suspended in buffer A (0.3 M sucrose, 25 mK HEPES, pH 7.5, 1 mM MgCl2), to yield a final Chl concentration of 1 mg $ml^{-1}$. Cells were then broken by sonication (Biologics, Inc., Model 300 V/T Ultrasonic Homogenizer, Manassas, VA, USA) five times for 10 sec each time (pulse mode, 50% duty cycle, output power 5) on ice. The unbroken cells were pelleted by centrifugation at 3000 ***g*** for 2 min at 4°C. The supernatant was centrifuged at 12 000 ***g*** for 20 min and the resulting pellet was washed with buffer A. The sample was subjected to a second centrifugation step at 11 000 ***g*** to collect thylakoids (Perrine *et al.*, 2012). Thylakoids containing 8 μg of chlorophyll were solubilized for 30 min by addition of equal volume of buffer containing β-dodecyl-maltoside at a 2% w/v concentration. 1/10 volume of sample buffer containing Serva-Blue G was added and the sample was centrifuged in a microfuge for 10 min at maximum speed. Thylakoid complexes were resolved for 6 h at 4°C on 4–12% Tris Tricine gel using Novex minigel system with a constant current of 6 mA as described by Järvi *et al.* (2011).

### SDS-PAGE and immunoblotting analysis

SDS-PAGE and immunoblotting for the LHCSR3 protein were conducted as described previously (Tokutsu and Minagawa, 2013). LHCSR3 protein expression was visualized using a commercial antibody (Eurogentec, Belgium) against LHCSR3 polypeptide (Naumann *et al.*, 2007).

### Transmission electron microscopy

Cells from all the lines were grown in low light (50 μmol photons $m^{-2}$ $sec^{-1}$) intensities for 5 days in HS medium in shaker flasks. Cells were prepared for electron microscopy by immobilizing cells in 3% sodium alginate (w/v) and the alginate beads were then solidified by incubation in cold 30 mM $CaCl_2$ for 30 min. Cells were encapsulated in alginate before chemical fixation. The encapsulated cells were fixed using 2% glutaraldehyde buffered with algal growth medium for 1.5–2 h. After fixation the cells were post-fixed in buffered 2% osmium tetroxide for 1.5 h and rinsed with water three times. Following dehydration in an ethanol-acetone dehydration series and after dehydration these cells were embedded in Spurr's resin. Thin sections were stained subsequently with uranyl acetate and lead citrate. An LEO 912 transmission electron microscope (ZEISS, USA) was used to view and collect images at 120 kV using a Proscan digital camera. Intracellular distances were measured on magnification-calibrated images using Fiji software (Image J). Distances reported are average of 150–200 measurements per cell line type.


## ACKNOWLEDGEMENTS

This work was jointly supported as part of the Photosynthetic Antenna Research Center (PARC), an Energy Frontier Research Center funded by the US Department of Energy, Office of Science, Basic Energy Sciences under award #DE-SC0001035, Bioenergy Technologies Office (BETO) funded REAP (Realization Of Algae Potential) DE-EE0006316, and PACE (Producing Algae for Coproducts and Energy) DE-EE0007089 (RS, SN). Enterprise Rent a Car Institute for Renewable Fuels, Donald Danforth Plant Science Center (RS, ZP and AK). US Air Force-Office of Scientific Research FA9550-08-1-0451 (Z P). Japan Society for the Promotion of Science, KAKENHI (16H06553, to JM); and the Ministry of Education, Culture, Sports, Science and Technology, through the Network of Centers of Carbon Dioxide Resource Studies in Plants (to JM); the DOE supported National Alliance for Advanced Biofuels and Bioproducts, contract EE00030406 (RS and AB) for ePBR purchasing; the Los Alamos National Laboratory (LANL) Laboratory Directed Research & Development (LDRD), award 20120535ER (AB, RS) for support of ePBR experiments; and the New Mexico Consortium and Pebble Laboratories for general support for materials and supplies and salaries. Lastly, GG was supported by the Schools of Integrative Biology and of Molecular and Cell Biology of the University of Illinois at Urbana-Champaign.


## AUTHOR CONTRIBUTIONS

RS conceived the idea for creation of self-adjusting antenna transgenics. SN designed and executed experiments for photosynthesis, growth, and biomass analysis, pigment analysis, and green native gel experiments. ZP and AK designed vectors, transformed algae, and performed initial screening for NC lines. JM and RT contributed in designing and executing photosystem II cross-section, NPQ, and LHCSR immunoblotting, AB contributed in ePBR experiment management. SN, NF, JM RS and GG contributed in interpretation of experiments and wring of the manuscript. RHB carried out electron microscopy work. All authors contributed in reviewing manuscript.

## CONFLICT OF INTEREST

Authors declare no competing financial interests.

## DATA AVAILABILITY STATEMENT

All original data and material information requests can be made to either Richard Sayre at richardtsayre@gmail.com or the Sangeeta Negi at sangeeta@newmexicoconsortium.org.

## SUPPORTING INFORMATION

Additional Supporting Information may be found in the online version of this article.

**Figure S1.** Correlation of optical density ($OD^{750}$) with cell number is shown. The optical density of the cultures was monitored on a daily basis at 750 nm using a Cary 300 Bio UV–visible light spectrophotometer (Agilent). Cell numbers were counted using an Accuri c6 flow cytometer (BD Biosciences). Values shown here are means ± SD ($n$ = 3).

**Figure S2.** Schematic drawing of the thylakoid membrane system. The distances of membrane bilayer (Granum), and lumen space are indicated as measured in transmission electron microscopy (TEM) images.

**Figure S3.** Comparative model for thylakoid membrane thickness and lumen space in wild-type and NC lines, showing diffusion of plastocyanin (PC) (see arrow). PQ, plastoquinone; PC, plastocyanin. (a) Wild-type, (b) NC lines.

**Table S1.** Chlorophyll and carotenoid content of select *Chlamydomonas* photosystem II and photosystem I light-harvesting complex protein subunits as determined from their cryo-EM structures (Sheng *et al.*, 2019; Suga *et al.*, 2019).

## REFERENCES


**Allen, J.F. and Forsberg, J.** (2001) Molecular recognition in thylakoid structure and function. *Trends Plant Sci.* **6**, 317–326.

**Arnon, D.I.** (1949) Copper enzymes in isolated chloroplasts. Polyphenoloxidase in *Beta Vulgaris*. *Plant Physiol.* **24**, 1–15.

**Ballottari, M., Mozzo, M., Croce, R., Morosinotto, T. and Bassi, R.** (2009) Occupancy and functional architecture of the pigment binding sites of photosystem II antenna complex Lhcb5. *J. Biol. Chem.* **284**, 8103–8113.

**Barber, J. and Chow, W.S.** (1979) A mechanism for controlling the stacking and unstacking of chloroplast thylakoid membranes. *FEBS Lett.* **105**, 5–10.

**Beckmann, J., Lehr, F., Finazzi, G., Hankamer, B., Posten, C., Wobbe, L. and Kruse, O.** (2009) Improvement of light to biomass conversion by de-regulation of light-harvesting protein translation in *Chlamydomonas reinhardtii*. *J. Biotechnol.* **142**, 70–77.

**Berman, G.P., Nesterov, A.I., López, G.V. and Sayre, R.T.** (2015) Superradiance transition and nonphotochemical quenching in photosynthetic complexes. *J. Phys. Chem C.* **119**, 22289–22296.

**Björkman, O. and Demmig, B.** (1987) Photon yield of $O_2$ evolution and chlorophyll fluorescence characteristics at 77 K among vascular plants of diverse origins. *Planta*, **170**, 489–504.

**Blankenship, R.E. and Chen, M.** (2013) Spectral expansion and antenna reduction can enhance photosynthesis for energy production. *Curr. Opin. Chem. Biol.* **17**, 457–461.

**Blankenship, R.E., Tiede, D.M., Barber, J. *et al.*** (2011) Comparing photosynthetic and photovoltaic efficiencies and recognizing the potential for improvement. *Science*, **332**, 805–809.

**Bonente, G., Ballottari, M., Truong, T.B., Morosinotto, T., Ahn, T.K., Fleming, G.R., Niyogi, K.K. and Bassi, R.** (2011) Analysis of LhcSR3, a protein essential for feedback de-excitation in the green alga *Chlamydomonas reinhardtii*. *PLoS Biol.* **9**, e1000577.

**Cao, M., Fu, Y., Guo, Y. and Pan, J.** (2009) *Chlamydomonas* (Chlorophyceae) colony PCR. *Protoplasma*, **235**, 107–110.

**Cazzaniga, S., Dall'Osto, L.Szaub, J., Scibilia, L., Ballottari, M., Purton, S. and Bassi, R.** (2014) Domestication of the green alga *Chlorella sorokiniana:* reduction of antenna size improves light-use efficiency in a photobioreactor. *Biotechnol. Biofuels*, **7**, 1–13.

**Chow, W.S., Kim, E.-H., Horton, P. and Anderson, J.M.** (2005) Granal stacking of thylakoid membranes in higher plant chloroplasts: the physicochemical forces at work and the functional consequences that ensue. *Photochem. Photobiol. Sci.* **4**, 1081–1090.

**Dall'Osto, L., Cazzaniga, S., Havaux, M. and Bassi, R.** (2010) Enhanced photoprotection by protein-bound vs free xanthophyll pools: a comparative analysis of chlorophyll b and xanthophyll biosynthesis mutants. *Mol. Plant*, **3**, 576–593.

**Demmig-Adams, B., Garab, G., Adams, W.W. III and Govindjee, G.** (eds). (2016) *Non-Photochemical Quenching and Energy Dissipation in Plants, Algae and Cyanobacteria. Advances in Photosynthesis and Respiration.* Volume 40. Dordrecht: Springer.

**Depège, N., Bellafiore, S. and Rochaix, J.-D.** (2003) Role of chloroplast protein kinase Stt7 in LHCII phosphorylation and state transition in *Chlamydomonas*. *Science*, **299**, 1572–1575.

**Drop, B., Webber-Birungi, M., Yadav, S.K.N., Filipowicz-Szymanska, A., Fusetti, F., Boekema, E.J. and Croce, R.** (2014) Light-harvesting complex II (LHCII) and its supramolecular organization in *Chlamydomonas reinhardtii*. *Biochim. Biophys. Acta Bioenerg.* **1837**, 63–72.

**Ducat, D.C. and Silver, P.A.** (2012) Improving carbon fixation pathways. *Curr. Opin. Chem. Biol.* **16**, 337–44.

**Eggink, L.L., LoBrutto, R., Brune, D.C., Brusslan, J., Yamasato, A., Tanaka, A. and Hoober, J.K.** (2004) Synthesis of chlorophyll b: localization of chlorophyllide a oxygenase and discovery of a stable radical in the catalytic subunit. *BMC Plant Biol.* **4**, 5.

**Formaggio, E., Cinque, G. and Bassi, R.** (2001) Functional architecture of the major light-harvesting complex from higher plants. *J. Mol. Biol.* **314**, 1157–1166.

**Formighieri, C., Franck, F. and Bassi, R.** (2012) Regulation of the pigment optical density of an algal cell: filling the gap between photosynthetic productivity in the laboratory and in mass culture. *J. Biotechnol.* **162**, 115–123.

**Friedland, N., Negi, S., Wu, G., Ma, L., Flynn, S., Cahoon, E., Lee, C.-H. and Sayre, R.T.** (2019) Tuning the photosynthetic light harvesting apparatus for improved efficiency and biomass yield. *Sci. Rep.* **9**(1), 13028.

**Gilmore, A.M., Hazlett, T.L., Debrunner, P.G. and Govindjee, G.** (1996a) Photosystem II chlorophyll *a* fluorescence lifetimes are independent of the antenna size differences between barley wild-type and chlorine mutants: comparison of xanthophyll cycle dependent and photochemical quenching. *Photosynth. Res.* **48**, 171–187.

**Gilmore, A., Hazlett, T.L., Debrunner, P.G. and Govindjee, G.** (1996b) Comparative time-resolved photosystem II chlorophyll a fluorescence analyses reveal distinctive differences between photoinhibitory reaction center damage and xanthophyll cycle dependent energy dissipation. *Photochem. Photobiol.* **64**, 552–563.

**Haehnel, W.** (1984) Photosynthetic electron transport in higher plants. *Annu. Rev. Plant Physiol.* **35**, 659–693.

**Havaux, M., Dall'osto, L. and Bassi, R.** (2007) Zeaxanthin has enhanced antioxidant capacity with respect to all other xanthophylls in *Arabidopsis* leaves and functions independent of binding to PSII antennae. *Plant Physiol.* **145**, 1506–1520.

**Holt, N.E., Zigmantas, D., Valkunas, L., Li, X.P., Niyogi, K.K. and Fleming, G.R.** (2005) Carotenoid cation formation and the regulation of photosynthetic light harvesting. *Science*, **307**, 433–436.

**Hoober, J.K., Eggink, L.L. and Chen, M.** (2007) Chlorophylls, ligands and assembly of light-harvesting complexes in chloroplasts. *Photosynth. Res.* **94**, 387–400.

**Järvi, S., Suorsa, M., Paakkarinen, V. and Aro, E.-M.** (2011) Optimized native gel systems for separation of thylakoid protein complexes: novel super- and mega-complexes. *Biochem. J.* **439**, 207–214.

**Johnson, M.P., Goral, T.K., Duffy, C.D., Brain, A.P., Mullineaux, C.W. and Ruban, A.V.** (2011) Photoprotective energy dissipation involves the reorganization of photosystem II light-harvesting complexes in the grana membranes of spinach chloroplasts. *Plant Cell.* **23**, 1468–1479.

**Kargul, J. and Barber, J.** (2008) Photosynthetic acclimation: structural reorganisation of light harvesting antenna - role of redox-dependent phosphorylation of major and minor chlorophyll a/b binding proteins. *FEBS J.* **275**, 1056–1068.

**Kargul, J., Turkina, M.V., Nield, J., Benson, S., Vener, A.V. and Barber, J.** (2005) Light-harvesting complex II protein CP29 binds to photosystem I of *Chlamydomonas reinhardtii* under State 2 conditions. *FEBS J.* **272**, 4797–4806.

**Kindle, K.L., Schnell, R.A., Fernández, E. and Lefebvre, P.A.** (1989) Stable nuclear transformation of *Chlamydomonas* using the *Chlamydomonas* gene for nitrate reductase. *J. Cell Biol.* **109**, 2589–2601.

**Kirchhoff, H.** (2014) Structural changes of the thylakoid membrane network induced by high light stress in plant chloroplasts. *Philos. Trans. R. Soc. Lond. B. Biol. Sci.* **369**, 20130225.

**Kirchhoff, H., Tremmel, I., Haase, W. and Kubitscheck, U.** (2004) Supramolecular photosystem II organization in grana thylakoid membranes: evidence for a Structured Arrangement†. *Biochemistry*, **43**, 9204–9213.

**Kirchhoff, H., Haferkamp, S., Allen, J.F., Epstein, D.B.A. and Mullineaux, C.W.** (2008) Protein diffusion and macromolecular crowding in thylakoid membranes. *Plant Physiol.* **146**, 1571–1578.

**Kirchhoff, H., Sharpe, R.M., Herbstova, M., Yarbrough, R. and Edwards, G.E.** (2013) Differential mobility of pigment-protein complexes in granal and agranal thylakoid membranes of $C_3$ and $C_4$ plants. *Plant Physiol.* **161**, 497–507.

**Kirst, H., Garcia-Cerdan, J.G., Zurbriggen, A., Ruehle, T. and Melis, A.** (2012) Truncated photosystem chlorophyll antenna size in the green microalga *Chlamydomonas reinhardtii* upon deletion of the TLA3-CpSRP43 gene. *Plant Physiol.* **160**, 2251–2260.

**Kromdijk, J., Głowacka, K., Leonelli, L., Gabilly, S.T., Iwai, M., Niyogi, K.K. and Long, S.P.** (2016) Improving photosynthesis and crop productivity by accelerating recovery from photoprotection. *Science*, **354**, 857–861.

**Kumar, A., Falcao, V.R. and Sayre, R.T.** (2013) Evaluating nuclear transgene expression systems in *Chlamydomonas reinhardtii*. *Algal Res.* **2**, 321–332.

**Lauk, C. and Lutz, J.** (2016) The future is made. Imagining feasible food and farming futures in an unpredictable world. In: *Land Use Competition.* Volume 6; Human-Environment Interactions. Berlin, Germany: Springer. pp. 233–246.

**Li, Z., Wakao, S., Fischer, B.B. and Niyogi, K.K.** (2009) Sensing and responding to excesslLight. *Annu. Rev. Plant Biol.* **60**, 239–260.

**Liguori, N., Roy, L.M., Opacic, M., Durand, G. and Croce, R.** (2013) Regulation of light harvesting in the green alga *Chlamydomonas reinhardtii*: the C-terminus of LHCSR is the knob of a dimmer switch. *J Am Chem Soc.* **135**, 18339–18342.

**Long, S.P., Humphries, S. and Falkowski, P.G.** (1994) Photoinhibition of photosynthesis in nature. *Annu. Rev. Plant Physiol. Plant Mol. Biol.* **45**, 633–662.

**Long, S.P., Long, S.P., Zhu, X.-G., Naidu, S.L. and Ort, D.R.** (2006) Can improved photosynthesis increase crop yields? Can improvement in photosynthesis increase crop yields? *Plant, Cell Environ.* **29**, 315–330.

**Minagawa, J.** (2011) State transitions—The molecular remodeling of photosynthetic supercomplexes that controls energy flow in the chloroplast. *Biochim. Biophys. Acta Bioenerg.* **1807**, 897–905.

**Mircovic, T., Ostrumov, E.E., Anna, J.M., van Grondelle, R., Govindjee, G. and Scholes, G.D.** (2016) Light absorption and energy transfer in the antenna complexes of photosynthetic organisms. *Chem. Rev.* https://doi.org/10.1021/acs.chemrev.6b00002.

**Mitra, M., Kirst, H., Dewez, D. and Melis, A.** (2012) Modulation of the light-harvesting chlorophyll antenna size in Chlamydomonas reinhardtii by TLA1 gene over-expression and RNA interference. *Philos. Trans. R. Soc. Lond. B. Biol. Sci.* **367**, 3430–3443.

**de Mooij, T., Janssen, M., Cerezo-Chinarro, O., Mussgnug, J.H., Kruse, O., Ballottari, M., Bassi, R., Bujaldon, S., Wollman, F.-A. and Wijffels, R.H.** (2015) Antenna size reduction as a strategy to increase biomass productivity: a great potential not yet realized. *J Appl. Phycol.* **27**, 1063–1077.

**Müller, P., Li, X.P. and Niyogi, K.K.** (2001) Non-photochemical quenching. A response to excess light energy. *Plant Physiol.* **125**, 1558–1566.

**Mullineaux, C.W.** (2005) Function and evolution of grana. *Trends Plant Sci.* **10**, 521–525.

**Mullineaux, C.W.** (2008) Factors controlling the mobility of photosynthetic proteins†. *Photochem. Photobiol.* **84**, 1310–1316.

**Mussgnug, J.H.** (2005) NAB1 is an RNA binding protein involved in the light-regulated differential expression of the light-harvesting antenna of *Chlamydomonas reinhardtii*. *Plant Cell*, **17**, 3409–3421.

**Mussgnug, J.H., Thomas-Hall, S., Rupprecht, J., Foo, A., Klassen, V., McDowall, A., Schenk, P.M., Kruse, O. and Hankamer, B.** (2007) Engineering photosynthetic light capture: impacts on improved solar energy to biomass conversion. *Plant Biotechnol. J.* **5**, 802–814.

**Nagy, G., Ünnep, R., Zsiros, O. *et al.*** (2014) Chloroplast remodeling during state transitions in *Chlamydomonas reinhardtii* as revealed by noninvasive techniques in vivo. *Proc. Natl Acad. Sci. USA*, **111**, 5042–5047.

**Natali, A. and Croce, R.** (2015) Characterization of the major light-harvesting complexes (LHCBM) of the green alga *Chlamydomonas reinhardtii*. *PLoS ONE*, **10**, e0119211.

**Naumann, B., Busch, A., Allmer, J., Ostendorf, E., Zeller, M., Kirchhoff, H. and Hippler, M.** (2007) Comparative quantitative proteomics to investigate the remodeling of bioenergetic pathways under iron deficiency in *Chlamydomonas reinhardtii*. *Proteomics*, **7**, 3964–3979.

**Nedbal, L., Trtílek, M. and Kaftan, D.** (1999) Flash fluorescence induction: a novel method to study regulation of Photosystem II. *J. Photochem. Photobiol. B Biol.* **48**, 154–157.

**Niinemets, U.** (2016) Within-canopy variations in functional leaf traits: structural, chemical and ecological controls and diversity of responses. In *Canopy Photosynthesis: From Basics to Applications* (Hikosaka, K., Niinemets, U. and Anten, N. P. R. eds). Adv. Photosynth. Resp. 42, Berlin, Germany: Springer, pp. 101–142.

**Niyogi, K.K.** (1999) PHOTOPROTECTION REVISITED: genetic and molecular approaches. *Annu. Rev. Plant Physiol. Plant Mol. Biol.* **50**, 333–359.

**Oey, M., Ross, I.L., Stephens, E., Steinbeck, J., Wolf, J., Radzun, K.A., Kü Gler, J., Ringsmuth, A.K., Kruse, O. and Hankamer, B.** (2013). RNAi knock-down of LHCBM1, 2 and 3 increases photosynthetic $H_2$ production efficiency of the green alga *Chlamydomonas reinhardtii*. *PLoS ONE*, **8**(4), e61375.

**Ohad, I., Prasil, O. and Adir, N.** (1992) Dynamics of photosystem II: mechanism of photoinhibition and recovery processes. In *The Photosystems.* Amsterdam, Netherlands: Elsevier, pp. 295–348.

**Olivares, J., Unkefer, C.J., Sayre, R.T. *et al.*** (2016) Review of the algal biology program within the National Alliance for Advanced Biofuels and Bioproducts. *Algal Res.* **22**, 187–215.

**Ort, D.R., Zhu, X.G. and Melis, A.** (2011) Optimizing antenna size to maximize photosynthetic efficiency. *Plant Physiol.* **155**, 79–85.

**Ort, D.R., Merchant, S.S., Alric, J. *et al.*** (2015) Redesigning photosynthesis to sustainably meet global food and bioenergy demand. *Proc. Natl Acad. Sci. USA*, **112**(28), 8529–8536.

**Peers, G., Truong, T.B., Ostendorf, E., Busch, A., Elrad, D., Grossman, A.R., Hippler, M. and Niyogi, K.K.** (2009) An ancient light-harvesting protein is critical for the regulation of algal photosynthesis. *Nature*, **462**, 518–521.

**Perrine, Z., Negi, S. and Sayre, R.T.** (2012) Optimization of photosynthetic light energy utilization by microalgae. *Algal Res.* **1**, 134–142.

**Polle, J.E.W., Benemann, J.R., Tanaka, A. and Melis, A.** (2000) Photosynthetic apparatus organization and function in the wild type and a chlorophyll b -less mutant of *Chlamydomonas reinhardtii*. Dependence on carbon source. *Planta*, **211**, 335–344.

**Polle, J.E.W., Kanakagiri, S.-D. and Melis, A.** (2003) tla1, a DNA insertional transformant of the green alga *Chlamydomonas reinhardtii* with a truncated light-harvesting chlorophyll antenna size. *Planta*, **217**, 49–59.

**Richard, C., Ouellet, H. and Guertin, M.** (2000) Characterization of the LI818 polypeptide from the green unicellular alga *Chlamydomonas reinhardtii*. *Plant Mol. Biol.* **42**, 303–316.

**Rochaix, J.-D.** (2007) Role of thylakoid protein kinases in photosynthetic acclimation. *FEBS Lett.* **581**, 2768–2775.

**Ruban, A.V.** (2015) Evolution under the sun: optimizing light harvesting in photosynthesis. *J. Exp. Bot.* **66**, 7–23.

**Ruban, A.V., Berera, R., Ilioaia, C., van Stokkum, I.H., Kennis, J.T., Pascal, A.A., van Amerongen, H., Robert, B., Horton, P. and van Grondelle, R.** (2007) Identification of a mechanism of photoprotective energy dissipation in higher plants. *Nature*, **450**, 575–578.

**Ruffle, S.V., Wang, J., Johnston, H.G., Gustafson, T.L., Hutchison, R.S., Minagawa, J., Crofts, A. and Sayre, R.T.** (2001) Photosystem II peripheral accessory chlorophyll mutants in *Chlamydomonas reinhardtii*. Biochemical characterization and sensitivity to photo-inhibition. *Plant Physiol.* **127**, 633–44.

**Sheng, X., Watanabe, A., Li, A., Kim, E., Song, C., Murata, K., Song, D., Minagawa, J. and Liu, Z.** (2019) Structural insight into light harvesting for photosystem II in green algae. *Nat. Plants*, **5**(12), 1320–1330.

**Sizova, I., Fuhrmann, M. and Hegemann, P.** (2001) A *Streptomyces rimosus* aphVIII gene coding for a new type phosphotransferase provides stable antibiotic resistance to *Chlamydomonas reinhardtii*. *Gene*, **277**, 221–229.

**Stephenson, A.L., Dennis, J.S., Howe, C.J., Scott, S.A. and Smith, A.G.** (2010) Influence of nitrogen-limitation regime on the production by *Chlorella vulgaris* of lipids for biodiesel feedstocks. *Biofuels*, **1**, 47–58.

**Su, X., Ma, J., Pan, X., Zhao, X., Chang, W., Liu, Z., Zhang, X. and Li, M.** (2019) Antenna arrangement and energy transfer pathways of a green algal photosystem-I-LHCI supercomplex. *Nat. Plants*, **5**, 273–281.

**Subramanian, S., Barry, A.N., Pieris, S. and Sayre, R.T.** (2013) Comparative energetics and kinetics of autotrophic lipid and starch metabolism in chlorophytic microalgae: implications for biomass and biofuel production. *Biotechnol. Biofuels*, **6**, 150.

**Suga, M., Ozawa, S.-I., Yoshida-Motomura, K., Akita, F., Miyazaki, N. and Takahashi, Y.** (2019) Structure of the green algal photosystem I supercomplex with a decameric light-harvesting complex I. *Nat. Plants*, **5**, 626–636.

**Takahashi, H., Iwai, M., Takahashi, Y. and Minagawa, J.** (2006) Identification of the mobile light-harvesting complex II polypeptides for state transitions in *Chlamydomonas reinhardtii*. *Proc. Natl Acad. Sci. USA*, **103**, 477–482.

**Tanaka, A., Ito, H., Tanaka, R., Tanaka, N.K., Yoshida, K. and Okada, K.** (1998) Chlorophyll a oxygenase (CAO) is involved in chlorophyll b formation from chlorophyll a. *Proc. Natl Acad. Sci. USA*, **95**, 12719–12723.

**Tian, L. and DellaPenna, D.** (2001) Characterization of a second carotenoid beta-hydroxylase gene from *Arabidopsis* and its relationship to the LUT1 locus. *Plant Mol. Biol.* **47**, 379–88.

**Tokutsu, R. and Minagawa, J.** (2013) Energy-dissipative supercomplex of photosystem II associated with LHCSR3 in *Chlamydomonas reinhardtii*. *Proc. Natl Acad. Sci. USA*, **110**, 10016–10021.

**Tokutsu, R., Iwai, M. and Minagawa, J.** (2009) CP29, a monomeric light-harvesting complex II protein, is essential for state transitions in *Chlamydomonas reinhardtii*. *J. Biol. Chem.* **284**, 7777–7782.

**Tremmel, I., Kirchhoff, H., Weis, E. and Farquhar, G.** (2003) Dependence of plastoquinol diffusion on the shape, size, and density of integral thylakoid proteins. *Biochim. Biophys. Acta Bioenerg.* **1607**, 97–109.

**Wang, Q., Zhang, Q.D., Zhu, X.G., Lu, C.M., Kuang, T.Y. and Li, C.Q.** (2002) PSII photochendstry and xanthophyll cycle in two superhigh-yield rice hybrids, Liangyoupeijiu and Hua-an 3 during photoinhibition and subsequent restoration. *Acta Bot. Sin.* **44**, 1297–1302.

**Wang, N., Fang, W., Han, H., Sui, N., Li, B. and Meng, Q.-W.** (2008) Overexpression of zeaxanthin epoxidase gene enhances the sensitivity of tomato PSII photoinhibition to high light and chilling stress. *Physiol. Plant.* **132**, 384–396.

**Whitmarsh, J. and Govindjee.** (1995) Photosynthesis. Encyclopedia of Applied Physics, **13**, 513–532.

**Witt, H.T.** (1971) Coupling of quanta, electrons, fields, ions and phosphorylation in the functional membrane of photosynthesis. Results by pulse spectroscopic methods. *Quart. Rev. Biophys.* **4**(4), 365–477.

**Wobbe, L. and Remacle, C.** (2015) Improving the sunlight-to-biomass conversion efficiency in microalgal biofactories. *J. Biotechnol.* **201**, 28–42.

**Wobbe, L., Blifernez, O., Schwarz, C., Mussgnug, J.H., Nickelsen, J. and Kruse, O.** (2009) Cysteine modification of a specific repressor protein controls the translational status of nucleus-encoded LHCII mRNAs in *Chlamydomonas*. *Proc. Natl Acad. Sci. USA*, **106**, 13290–13295.

**Wollman, F.A.** (2001) State transitions reveal the dynamics and flexibility of the photosynthetic apparatus. *EMBO J.* **20**, 3623–3630.

**Yamazaki, J.-Y., Suzuki, T., Maruta, E. and Kamimura, Y.** (2005) The stoichiometry and antenna size of the two photosystems in marine green algae, *Bryopsis maxima* and *Ulva pertusa*, in relation to the light environment of their natural habitat. *J. Exp. Bot.* **56**, 1517–1523.

**Zhu, X.-G., Long, S.P. and Ort, D.R.** (2008) What is the maximum efficiency with which photosynthesis can convert solar energy into biomass? *Curr. Opin. Biotechnol.* **19**, 153–159.


*The Plant Journal*, (2020), doi: 10.1111/tpj.14751